Environ. Sci. Technol. **2005**, *39,* 4767−4783

Summertime Ambient Formaldehyde in Five U.S. Metropolitan Areas: Nashville, Atlanta, Houston, Philadelphia, and Tampa

PURNENDU K. DASGUPTA,*,† JIANZHONG LI,† GENFA ZHANG,† WINSTON T. LUKE,‡ WILLIAM A. MCCLENNY,§ JOCHEN STUTZ,|| AND ALAN FRIED⊥

Department of Chemistry, Texas Tech University, Lubbock, Texas 79409-1061, NOAA/Air Resources Laboratory, R/E/AR, SSMC3, 1315 East-West Highway, Silver Spring, Maryland 20910, U.S. EPA, MD-205-03, 109 Alexander Drive, Research Triangle Park, North Carolina 27711, Department of Atmospheric and Oceanic Sciences, University of California, Los Angeles, California 90095-1565, and Atmospheric Technology and Chemistry Divisions, National Center for Atmospheric Research, Boulder, Colorado 80303

First, we briefly review the atmospheric chemistry and previous intercomparison measurements for HCHO, with special reference to the diffusion scrubber Hantzsch reaction based fluorescence instrument used in the field studies reported herein. Then we discuss summertime HCHO levels in five major U.S. cities measured over 1999−2002, primarily from ground-based measurements. Land−sea breeze circulations play a major role in observed concentrations in coastal cities. Very high HCHO peak mixing ratios were observed in Houston (>47 ppb) where the overall median mixing ratio was 3.3 ppb; the corresponding values in Atlanta were ∼>18 and 7.9 ppb, respectively. The peak and median mixing ratios (9.3 and 2.3 ppb) were the lowest for Tampa, where the land−sea breeze also played an important role. In several cities, replicate HCHO measurements were made by direct spectroscopic instruments; the instruments were located kilometers from each other and addressed very different heights (e.g., 106 vs 10 m). Even under these conditions, there was remarkable qualitative and often quantitative agreement between the different instruments, when they were all sampling the same air mass within a short period of each other. Local chemistry dominates how HCHO is formed and dissipated. The high concentrations in Houston resulted from emissions near the ship channel; the same formaldehyde plume was measured at two sites and clearly ranged over tens of kilometers. Local micrometeorology is another factor. HCHO patterns measured at a high-rise site in downtown Nashville were very much in synchrony with other ground sites 12 km away until July 4 celebrations whence HCHO concentrations at the downtown site remained elevated for several days and nights. The formation and dissipation of HCHO in the different cities are discussed in terms of other concurrently measured species and meteorological vectors. The vertical profiles of HCHO in and around Tampa under several different atmospheric conditions are presented. The extensive data set represented in this paper underscores that urban HCHO measurements can now be made easily; the agreement between disparate instruments (that are independently calibrated or rely on the absolute absorption cross section) further indicates that such measurements can be done reliably and accurately for this very important atmospheric species. The data set presented here can be used as a benchmark for future measurements if the use of formaldehyde precursors such as methanol or methyl *tert*-butyl ether (MTBE) as oxygenated fuel additives increases in the future.

* Corresponding author e-mail: Sandyd@ttu.edu.
† Texas Tech University.
‡ NOAA/Air Resources Laboratory.
§ U.S. EPA.
|| University of California.
⊥ National Center for Atmospheric Research.

1. Introduction

Formaldehyde is the most abundant tropospheric carbonyl compound and plays a pivotal role in atmospheric chemistry. Among primary natural sources of HCHO, animal excretion makes the biggest contribution (*1*), but overall this contribution is insignificant. There are also diverse anthropogenic primary sources, ranging from production of petrochemicals to processing of coal, manufacturing of plastics, paints, and varnishes, and sewage treatment to coffee roasting (*1*−*2*). Biomass burning, both natural (e.g., forest fires) and deliberate incineration, emit HCHO (*1*−*6*). The incomplete combustion of fossil fuels results in HCHO: it is present at high levels in auto exhaust (*7*−*8*). Ironically, "clean fuels" such as natural gas produce particularly significant levels (*9*−*10*). In large-bore gas turbine engine exhaust, the ratio of HCHO to total hydrocarbons in the exhaust is ∼1−2.5% (*11*). Exhaust from internal combustion engines powered by sludge digester gas contains 50−200 ppm HCHO (*12*). Formaldehyde generation can become an issue with other clean power generation technologies of the future. Methanol-based fuel cells, which many regard as ultimately more practical than hydrogen fuel cells, can produce substantial amounts of HCHO (*13*−*14*).

In urban areas, primary emissions from automotive exhaust can be a major contributor to observed HCHO. In downtown Denver in the summer, HCHO levels peak before noon, suggesting the dominance of automotive sources (*7*). In Denver, Anderson et al. also noted an increase in HCHO levels as greater oxygenate content in fuel was implemented (*7*). Using more widely distributed sampling sites (six locations within beltway I-270), Mukund et al. (*15*) found primary automotive emissions to account for 17% of the observed HCHO in Columbus, OH (1989 population ∼1 million) even before oxygenates were used in fuel. However, primary emission sources globally account for a small fraction of the atmospheric HCHO. In North America, primary emissions account for ∼<5% of the observed HCHO. The rest is produced by atmospheric photochemical oxidation of hydrocarbons (*16*). Almost all volatile organic compounds (VOCs) form some carbonyl compounds upon photooxidation to a degree (*1*): the HCHO formation potential of several VOCs was quantitatively evaluated in the 1995 Nashville study (*17*). During the growing season, isoprene from vegetation is the dominant HCHO precursor (*18*). Satellite observations of North America during the global ozone monitoring experiment provided images of HCHO columns; for the southeastern United States in the summertime this can be regarded as a de facto isoprene emission map.

10.1021/es048327d CCC: $30.25
Published on Web 05/28/2005

In the background atmosphere, methane is the primary precursor of HCHO (*19*); CH_4 is converted to $^{\bullet}CH_3$ upon H-abstraction by $^{\bullet}OH$ and thence to $CH_3OO^{\bullet}$ by reaction with O_2. The $CH_3OO^{\bullet}$ can be converted to HCHO in one of three pathways, involving (a) CH_3OOH, (b) $CH_3O^{\bullet}$, and (c) CH_3OH, and thence $^{\bullet}CH_2OH$ (see Frost et al. (*20*)). Formaldehyde is lost in a number of pathways. It is oxidized by $^{\bullet}OH$ to $^{\bullet}CHO$ or photolyzed to H_2 and CO (λ < 365 nm) or to $H^{\bullet}$ and $^{\bullet}CHO$ (λ < 337 nm). Both $H^{\bullet}$ and $^{\bullet}CHO$ produce $HO_2^{\bullet}$ upon reaction with O_2 and thus HCHO acts as an important radical source. The recombination of two $HO_2^{\bullet}$ moieties to form H_2O_2 which can itself be photolyzed to form radicals then provides a further radical reservoir. The loss of HCHO can thus result in the formation of H_2O_2. When HCHO dissolves in atmospheric water, aqueous phase oxidation by various oxidants, notably $HO_2^{\bullet}$, converts HCHO to formic acid, widely found in ambient air and rain (*21*). Formaldehyde in atmospheric water in SO_2-rich environments also forms a reservoir for both HCHO and S(IV) in the form of hydroxymethanesulfonic acid, a unique constituent of fogwater (*22*−*24*). The lifetime of HCHO in the sunlit troposphere is limited to 2−4 h and elevated HCHO concentrations provide a good indicator of recent oxidation of volatile organic compounds (VOCs) (*25*).

In brief, HCHO is a key indicator of atmospheric photochemical activity. Although some early data for 10-day long periods have been reported (*26*), continuous measurement methods for HCHO of sufficient sensitivity have largely matured during the last 5 years when reasonable agreement between different instrumental techniques has been repeatedly established. Consequently, some measure of reliability is now assured. With rare exceptions (*27*), sustained measurements of HCHO over several week-long periods in major urban areas have not been reported, especially in the United States. We report here continuous ground-based HCHO measurements in 5 major U.S. cities (and vignettes of aircraft data from one location) over sustained, several-week-long periods, primarily obtained with a Nafion membrane diffusion scrubber (NMDS) instrument utilizing fluorometric Hantzsch cyclization chemistry in conjunction with relevant atmospheric chemistry and meteorology data. In several locations, direct spectroscopic HCHO measurements were available and are reported.

Formaldehyde Measurement Methods and Intercomparison Studies. Many HCHO measurement methods have been reported; more recent developments have been addressed in a recent review (*28*). Methods that are capable of short time resolution and which have actually been used to a significant extent in ambient air studies include gas-phase spectroscopic techniques, notably tunable diode laser absorption spectroscopy (TDLAS (*25*−*33*)) and differential optical absorption spectroscopy (DOAS (*34*−*36*)). TDLAS in particular has also been used in very-low-level background air measurements. Proton transfer reaction mass spectrometry (PTRMS) can also be used to measure HCHO simultaneously with many other species with fast time resolution, although the limit of detection for formaldehyde at 1−2 ppb is considerably poorer than that of most other compounds measured by PTRMS (*37*). Other approaches involve collection with derivatization, e.g., scrubbing in a glass coil and continuously (a) performing enzyme-based fluorescence detection (EFD) by *formaldehyde dehydrogenase* mediated reduction of nictotinamide adenine dinucleotide (NAD) to fluorescent NADH (*5*, *38*−*39*), or (b) derivatizing with dinitrophenylhydrazine and storing 3−5-min aliquots for subsequent analysis by high-performance liquid chromatography (Coil−DNPH−HPLC) (*17*, *20*, *40*), or (c) performing the Hantzsch reaction with ammonium acetate and a β-diketone (typically acetylacetone) and detecting the resulting fluorescent product (Coil−Hantzsch) (*41*). This last technique has become available as a commercial instrument (Aero-Laser GmbH) (*42*). A variant of (b) above using a porous membrane diffusion scrubber (PMDS) as a collector and coupled periodic HPLC analysis has also been used (*43*). The first automated fluorometric approach, based on the Hantzsch reaction, involved a PMDS collector (*44*); this is the approach we have refined and extensively used over the years with a Nafion membrane DS collector (Nafion DS−Hantzsch, NDSH) (*28*). This technique has also become available as a commercial instrument (Alpha-Omega Power Technologies) (*45*).

The first significant intercomparison of HCHO instrumentation took place in 1986 and involved TDLAS, EFD, and PMDS−Hantzsch methods along with cartridge and impinger collection based DNPH−HPLC (*46*). None of the methods showed obvious interferences from O_3, NO_2, SO_2, or H_2O_2. However, even in zero air the methods agreed overall with each other to only within ∼30%. A few months later the same instruments were tested for 11 days along with an open path Fourier transform infrared (FTIR) spectrometer (25-m base path, 1.15-km total path length) and an 800-m base path DOAS in Los Angeles (*26*). The PMDS−Hantzsch instrument produced results essentially identical to the mean of the direct spectroscopic instruments for the first few days but the observed results slowly became lower thereafter compared to the direct spectroscopic mean. Overall the EFD and PMDS−Hantzsch instruments produced values that were ∼25% higher and lower than the spectroscopic mean values, respectively. Later studies revealed that the early PMDS collectors (with nanometer-size pores) were particularly susceptible to fouling by deposited fine particles, leading to gradual loss of collection efficiency. Nevertheless, in September 1993, the same PMDS−Hantzsch method was deployed in the tropical savannah in Venezuela and compared against a DNPH-coated silica gel method with subsequent HPLC analysis (*47*). Over a range of 0.2−2 ppb, the two methods were reasonably correlated (linear r^2 0.80) with a slope statistically indistinguishable from unity (1.02±0.03). During the1993 $^{\bullet}OH$ photochemistry experiment (*36*), a 20.6-km-path DOAS was compared with a TDLAS over a 6-week period. The DOAS results were on the average 15% greater than those of the TDLAS, due to its proximity to anthropogenic sources. During periods of strong westerly flow where anthropogenic and meteorological influences were minimized, both techniques were in agreement to within 5% (*36*). In 1996, Mücke et al. (*39*) reported an intercomparison of a 27-m-path TDLAS with an EFD system. For 0−8 ppb calibration gas, the agreement was excellent (r^2 = 0.9997, slope 1.02±0.02), but with a simulated real sample consisting of a mixture of outdoor and indoor air (0−15 ppb), it was more modest (r^2 = 0.9180). The HCHO data from the TDLAS and the Coil−DNPH−HPLC system on 8 aircraft flights from the 1997 North Atlantic regional experiment were compared (*40*); the two instruments agreed to within ±0.1 ppbv. However, differences larger than the combined 2σ total uncertainty estimate were observed 29% of the time.

Cardenas et al. (*41*) have compared a TDLAS, two DOAS instruments, and an acetylacetone (2,4-pentanedione,PD)-based coil-Hantzsch instrument at a clean maritime site (HCHO < 1 ppbv). The best agreement was between the DOAS and the coil−Hantzsch instrument. The two DOAS instruments and the Coil−Hantzsch instrument were then compared on the north coast of England (HCHO up to 4 ppb); again, very good agreement was observed. The TDLAS and the Coil−Hantzsch instrument were compared in a mobile lab with varying degrees of indoor/outdoor mixing ratios: the correlation coefficient was 0.99.

Beginning in 1991, as the particle deposition and membrane blockage problem was better understood, the PMDS design was abandoned in favor of a hydrophilic Nafion membrane which had no physical pores to be blocked and

TABLE 1. Summary Statistics for Ground-Based HCHO Data with NDSH Instrument

study period	location[a]	no. valid ambient measurements (% coverage)	total rainfall, mm	HCHO, ppb max	HCHO, ppb min	HCHO, ppb mean	HCHO, ppb median
06/26/99 to 07/07/99	36.12°N 86.68°W Nashville, TN[b,c] Alt. 180 m	1469 (91.9%)	52.1	12.67	1.43	5.05	4.78
08/03/99 to 08/31/99	33.78°N: 84.41°W Atlanta, GA[d] Alt. 265 m	3550 (90.4%)	119.6	18.25	0.42	7.96	7.82
08/12/00 to 9/25/00	29.76_5°N 95.18°W Houston, TX[c,e] Alt. 6 m	6060 (96.4%)	164.3	47.13	0.15	4.49	3.30
06/27/01 to 07/31/01	40.04°N 75.00_5°W Philadelphia, PA[f] Alt. 8 m	4696 (96.4%)	33.0	9.53	0.33	3.12	2.89
04/25/02 to 06/01/02	27.96°N 82.23°W Sydney, FL[g] Alt. 30 m	5194 (97.7%)	27.2	9.38	0.37	2.63	2.32

[a] Altitude above mean sea level at ground level. [b] See http://www.al.noaa.gov/WWWHD/Pubdocs/SOS/SOS99.html for a description of the Nashville study. [c] All data from the supersite are available from the NOAA ftp site, ftp.al.noaa.gov; contact Eric.J.Williams@noaa.gov. [d] Site details are available from http://www-wlc.eas.gatech.edu/supersite/; contact Jim St. John (Stjohn@eas.gatecth.edu) for access to the archived data. [e] See http://www.utexas.edu/research/ceer/texaqs/ for the detailed description of the study and the experimental sites. [f] See http://lidar1.ee.psu.edu/neopsWeb/publicSite/narsto-neops/neops.htm for site details; contact C. Russell Philbrick (crp3@psu.edu) for access to archived data. [g] See http://www.hsc.usf.edu/publichealth/EOH/BRACE/ for the details of the BRACE study; contact Noreen Poor at npoor@hsc.usf.edu.

where the acidic hydrophilic nature of the membrane permitted better collection efficiency. Further, a straight, rather than a right-angled, geometry of the sample inlet/outlet greatly decreased particle deposition in the DS (*48*). Other than the inclusion of a thermostated enclosure, this design continues to date. PD had been used in the Hantzsch reaction chemistry throughout. In 1994, this was replaced with 1,3-cyclohexanedione (CHD) producing an order of magnitude improvement in sensitivity and limits of detection (LOD) (*49*). It is in this form that the NDSH instrument was deployed in the 1995 summer intercomparison in Boulder, CO hosted by the National Center for Atmospheric Research (NCAR) alongside TDLAS, EFD, Coil−DNPH−HPLC, and two other cartridge-based DNPH−HPLC methods using blind standards, zero and interferent gases/gas mixtures, and ambient air (*50*). None of the continuous methods showed any interference from O_3, SO_2, NO_2, or isoprene. Using linear regression results from a blind standards comparison (with the TDLAS as reference) to normalize all ambient results, the respective slopes relative to the TDLAS were 0.82±0.08, 1.04±0.14, and 1.00±0.11 for EFD, DNPH-HPLC, and NDSH, respectively (*50*, *51*).

The emergence of liquid core waveguide (LCW)-based fluorescence detection in 1999 greatly simplified the fluorescence detector design and permitted the use of near-UV light-emitting diodes (LEDs) for fluorescence detection in the CHD-based Hantzsch chemistry (*52*). A compact instrument of this type (*53*) was used in the 1999 Nashville and Atlanta studies reported here.

Researchers interested in exploiting the much greater sensitivity of the CHD-based Hantzsch reaction chemistry (compared to PD-chemistry) for HCHO measurements in relatively pristine polar samples noticed, however, a small positive interference from H_2O_2 (*54*−*56*). The error would be negligible in urban areas where the HCHO/H_2O_2 ratio is high. However, in the polar regions, HCHO(g) mixing ratios are very low (100−700 pptv) (*57*−*58*), while H_2O_2(g) mixing ratios have been reported to range from quite low (≤400 pptv) to significant summertime levels (0.5−3 ppb). Because of the vastly larger Henry's law constant for H_2O_2, the corresponding concentrations in snowmelt typically range from 3 to 30 μM H_2O_2 and 20−140 nM HCHO (*55*−*57*). In such samples, the worst case H_2O_2 interference can be significant, up to 40%. To attain general applicability, the chemistry was once again switched to PD from CHD, and almost the same sensitivity and LOD as that of the CHD system were attained by better detector design and brighter, multiple LED sources for fluorescence excitation. The PD-based chemistry was verified to have no interference from H_2O_2 and this is the format (*28*) in which the instrument was used in Houston (2000), Philadelphia (2001), and Tampa (2002). The instrument deployed on the aircraft in Tampa was redesigned in a rack-mount configuration with reduced weight and power consumption (*28*): in particular, it incorporated an energy-efficient self-regulating wire-in-tube heater to heat the reaction mixture (*59*).

Experimental Section

Site Description, Experiment Duration, and Sampling Details. Summary information about each of the study locations, duration, and percent coverage, and a skeleton summary of the NDSH instrument data are presented in Table 1. In all ground-based measurements, the NDSH instruments were operated on a 3-min sample, 7-min zero cycle, thus producing one measurement and a zero every 10 min. Further site details are given below.

Nashville. The NDSH instrument was located on the penthouse of the Polk Building in downtown Nashville during the Nashville supersite experiment. The sampling inlet was 106 m above ground level. The sample was drawn through a 2.5-cm diameter PFA Teflon manifold from the roof area of the building and resulted in a residence time of a few seconds. The NDSH instrument sampled at its specified flow rate (~1 L/min) from this manifold off a tee. The instrument was calibrated daily using zero air dilution of a calibration gas from a certified standard gas cylinder containing 5 ppmv of HCHO in N_2. Cross validation of this standard by the NCAR TDLAS instrument calibrated using a NCAR HCHO permeation tube standard indicated agreement within 3%. The NCAR TDLAS was located at Cornelia Fort Airpark (CFA), 12 km NE of the Polk Building. The DOAS instrument operated by the University of California at Los Angeles (UCLA) group was also located at CFA. Nashville site descriptions and DOAS details (the beam path was from Cornelia Fort to the Gaylord Building, 1.36 km away) are available elsewhere (*60*, *61*). The

NCAR TDLAS has been described in several publications already cited above.

Atlanta. The NDSH instrument was deployed in the Atlanta Supersite experimental site located on Jefferson Street in midtown Atlanta. Adjacent to the site was a bus repair depot and the site was occasionally impacted by diesel engine exhaust from this source. There were also frequent occurrences of midnight street-racing in the immediate vicinity, contributing to an unusual nighttime auto exhaust source. In Atlanta, as well as Houston, a Teflon-coated Al cyclone (designed for a 2.5-μm cut point at a flow rate of 3 L/min, URG, Chapel Hill, NC) with a downward pointing inlet ~2 m above the roof of the shelter (~6 m above ground) was used to remove coarse particles. The inlet conduit from the cyclone to the DS was PFA Teflon (5 mm i.d.). The total flow rate through the sampling system was 2.7 standard liters per minute (SLPM): 1.1 SLPM sampled by the present instrument and 1.6 SLPM sampled by a peroxide measurement instrument. The residence time in the sampling line was ~2 s. The sampling line was wrapped with aluminum tape (grounded to reduce aerosol deposition) to prevent light exposure. The instrument sensitivity was calibrated daily with aqueous standards and weekly with gaseous standards. The cyclone and the entire sample inlet line were washed weekly with deionized water and dried with compressed nitrogen to remove any deposited particles. Any calibration shift (always <15%) was compensated for by linear interpolation of the calibration data bracketing the sampling interval. The same calibration and maintenance protocol/frequency were followed for all of the ground-based measurements below.

Houston. As part of the Texas Air Quality Study 2000 (TEXAQS2000) experiments, the instrument was deployed at site HRM-3 (Houston Regional Monitoring Network, EPA site 48-201-0803) located at $1504^1/_2$ Haden Rd. This site is typically downwind from the heavily industrialized area of the Houston ship channel (9 km ESE of site) and in the midst of a petrochemical and a chemical manufacturing complex where contributions from primary emissions can occasionally be significant. The HRM-3 site is a permanent location for meteorological and criteria pollutant measurement instrumentation operated by the Texas Commission on Environmental Quality; the data from this site are web-accessible (*62*). The UCLA multipath DOAS instrument (*25*, *63*) was located at La Porte Airport, adjacent to the ship channel, 24 km SE from HRM-3.

Philadelphia. The North East Oxidant and Particle Study (NEOPS) 2001 site was located on the premises of the City of Philadelphia's Baxter water treatment plant in NE Philadelphia. The site is ~13 km NE of the city center and is located between I-95 and the Delaware river. Both in Philadelphia and Tampa, the sampling arrangement consisted of a 15-cm-diameter PVC pipe vertically traversing the shelter and extending 1 m above the rooftop with a U-joint on top to prevent precipitation ingress. Underneath the shelter, a blower fan was attached to the PVC pipe to aspirate air at 1000−1400 L/min, sufficiently fast to minimize wall losses or contributions from any wall emissions. A PFA Teflon tube, 3 mm i.d., breached the PVC pipe at a convenient height within the shelter with the end of the Teflon tube located at the center of the PVC pipe and angled downward. This arrangement effectively discriminated against large particles; no cyclone was used. Fluid dynamics calculations using the duct diameter and the sampling rate indicated that at the center, the flow stream is unaffected at the tapping point.

Tampa. Formaldehyde measurements were carried out as part of the Bay Region Atmospheric Chemistry Experiment (BRACE). The Sydney Supersite was rural, within the premises of the Valrico wastewater treatment plant, 22.5 km E of downtown Tampa.

Airborne experiments were conducted in Tampa aboard the NOAA Twin Otter aircraft on 21 separate flights, generally taking off from Vandenberg airport, ~13 km NE of downtown Tampa. The flights were typically 4−4.5 h in duration. The instrument was calibrated and zeroed immediately before and after the flight; calibration shifts generally amounted to ≤2%. Although the data aboard the aircraft were acquired continuously at a rate of 1 Hz, the 10−90% response time of the instrument was 2 min. A forward-facing inlet system was used to duct ambient air into the Twin Otter cabin for trace gas sampling. The inlet system consisted of a 90-cm length of 0.953-cm PFA Teflon tubing catheterized inside a reinforced, forward-facing inlet mounted on the forward-most window on the starboard side of the aircraft. The inlet tip terminated 3.4 m behind the nose of the aircraft and protruded approximately 15 cm above the fuselage surface. This position was judged to be most free of potential sources of contamination, and is forward of both the engine exhaust and the propeller line. The inlet tubing was cleaned periodically and replaced once during the study to ensure a clean sampling path. Both the inlet tip and manifold exhaust port were capped when the aircraft was not in flight. Flights were conducted in clear air only, thus there was no liquid water intrusion into the forward-facing inlet. The inlet tubing terminated in a longer section of 1.27-cm o.d., 2.1-m long PFA Teflon manifold. At normal cruising speeds of 55 m/s, the flow rate through the manifold was approximately 54 LPM (residence time ~0.1 s). Both the HCHO instrument and a H_2O_2 instrument (also using a NMDS) sampled off this manifold via short sections of 0.635-cm o.d. PFA tubing.

Auxiliary Measurements. With the exception of Nashville, H_2O_2 was measured at all sites. In Philadelphia and Tampa organic peroxides (mostly methyl hydroperoxide) were also measured with a dual-channel DS-fluorescence instrument. All peroxides were measured with 10-min time resolution (*64*). At all sites except Nashville, acid gases and particulate anionic constituents were measured with 15-min time resolution with a wet denuder−hydrophobic filter reflux particle collector system (*65*, *66*). At all sites, measurements of NO, O_3, and CO were made using commercial instruments according to established Federal reference/equivalent methods.

For the Tampa aircraft study, SO_2 was measured with a modified commercial instrument. Nitric acid measurements were recorded as the difference between two O_3-chemiluminescence NO monitors each equipped with a heated molybdenum NO_y converter, where one of the units contained a NaCl-coated denuder in the inlet to selectively remove HNO_3. Although the inlet losses at the sampling rate used have been observed to be negligible, the measured value should be considered the lower limit of the actual HNO_3 concentration.

Results and Discussion

Overview. Figure 1 presents an overview of the results, and, in conjunction with Table 1, summarizes measured HCHO values in four southern/southeastern cities and one northeastern city in the United States. Tampa, Philadelphia, and Nashville maxima range between just under 10 ppb to just under 13 ppb, quite comparable to the ~13 ppb maximum measured during the recent NITROCAT study in summer 2001 in Rome, Italy (*67*) (albeit studies in Rome in the 1990s have reported maximum mixing ratios of 27−28 ppb (*68*, *69*) and similarly high maxima have been reported for Athens, Greece in 2000 (*70*)). With an ~18 ppb maximum, Atlanta is significantly higher than the three aforementioned U.S. cities. Houston, with a maximum mixing ratio >47 ppb measured at both the HRM-3 and the La Porte sites, falls in a class by itself (this exceeds the reported maximum of 34 ppb from Milan in 1998 (*27*) and is second only to the reported

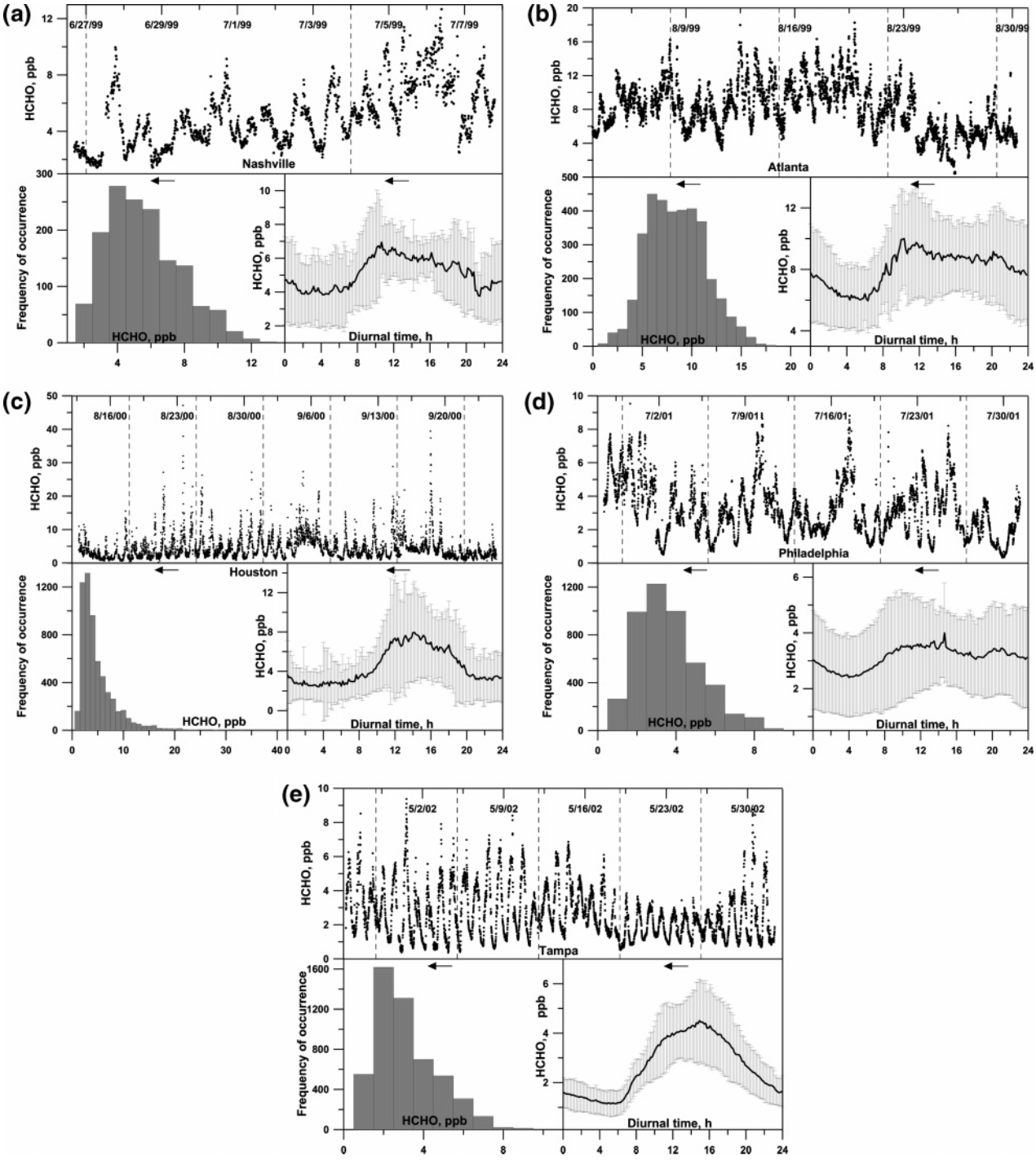

FIGURE 1. Ground level measurement overview, NDSH instrument: (a) Nashville, (b) Atlanta, (c) Houston, (d) Philadelphia, and (e) Tampa. The top panels show the mixing ratio data (vertical dashed lines indicate Sundays), the bottom panels show (left) histogram of the 10-min average data and (right) the diurnal variation with the average as the heavy trace and ±1 standard deviation error bars.

maximum of 54 ppb in a high traffic street in Rio de Janeiro (*71*); however, the maximum average daily peak concentration at that site was below those of Nashville, Atlanta, and Houston). The Houston maximum is, in fact, more than twice the peak concentrations measured in urban Los Angeles in the mid-1980s (*43*). Interestingly, Houston showed both the maximum and minimum values measured in any of the five cities; in terms of either mean or median values, Houston was below Atlanta and Nashville. In assimilating these results, it should be noted that the sampling sites in Nashville and Atlanta were in the middle of the city while those in Tampa and Philadelphia were at a substantial distance from the city center. The Houston sampling location was distant from the city center but close to the ship channel where much of the highly reactive VOC emissions in that city are known to originate. Further, at the time of the respective studies, oxygenated additives were mandated requirements in Houston and Philadelphia in the summertime. The histograms (Figure 1) and the mean vs median values (mean always higher than median values) in Table 1 indicate a tailing rather than a symmetric distribution around the median value.

The total rainfall record during the study periods followed the order of the listing in Table 1, with the average precipitation in mm/day during the study period correspondingly being 4.69, 4.38, 3.76, 0.98, and 0.74, with the month of May 2002 in Tampa being one of the driest on

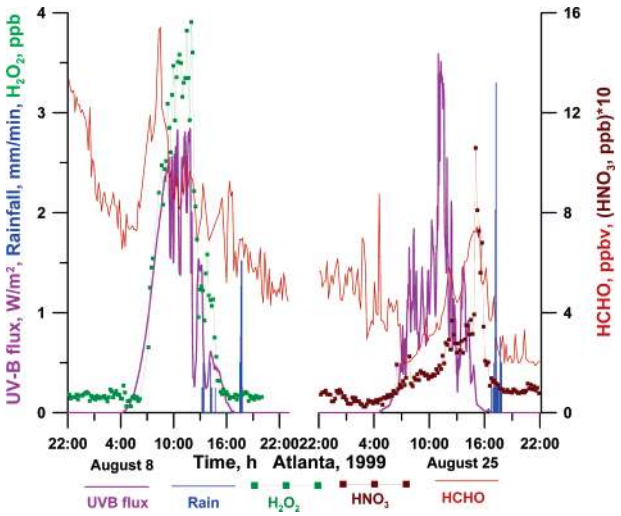

FIGURE 2. UV−B flux (violet) and rainfall intensity (blue) on two occasions in Atlanta along with HCHO concentration (red dots). These data suggest poor washout efficiency for HCHO in contrast to H_2O_2 (green) or HNO_3 (brown).

record. The lowest observed mixing ratio in Houston, 150 ppt, was not observed as a result of rainout; indeed the lowest value recorded on a day of torrential rainfall (48.3 mm, September 13, 2000) was ~1 ppb. In Figure 2, UV−B flux, rainfall, and HCHO concentrations are shown for two rain events in Atlanta. Both photochemical formation of HCHO and its photolytic loss processes cease as the UV is extinguished. These data clearly indicate that HCHO is washed out very inefficiently, in contrast to, e.g., HNO_3 or H_2O_2, for which we see obvious washout patterns (the decrease in concentration actually begins just before the recorded rainfall, possibly because of two reasons: (a) the onset of enhanced vertical mixing, and (b) the presence of atmospheric liquid water which is not yet sufficient to trip the rain collector). On August 25, the HCHO mixing ratio begins decreasing significantly before rainfall begins and shows sporadic increases during and after the rainfall. Dew, often in heavy amounts, was a daily occurrence in almost all the sites, especially in Nashville, Atlanta, and Philadelphia, but HCHO was not removed to near-zero levels during these periods.

Clear diurnal patterns for HCHO are generally observed in all the sites. The return to near-background values overnight before producing a mid-afternoon maximum is most clearly observed in the Houston and Tampa data. The overall diurnal variation in the mixing ratio (peak to valley) is least for Philadelphia. The pattern is also less striking in Nashville and to some extent Atlanta, where continuous isoprene production from green vegetation continues to produce HCHO throughout the day and removal of HCHO is not efficient in the absence of light overnight. Land−sea breeze recirculation patterns play a role in the overnight disappearance of HCHO in Houston (and to a lesser extent in Tampa). Figure 3 shows illustrative changes in wind direction at the HRM-3 location in Houston and more random circulatory patterns in Tampa. More detailed examination of each city follows.

Nashville. A more detailed description of many aspects of the 1999 Nashville study is available elsewhere (*72*). Three independent instruments measured HCHO during this study. Note that while the NDSH instrument was located at the top of the Polk Building (106 m in height) downtown, the other two instruments were located ~12 km downwind at the surface at CFA. The DOAS (x) vs TDLAS (y) data at the CFA site (slope 1.06 ± 0.04, intercept 0.15 ± 0.13 ppb, $n = 1010$) showed excellent agreement (*30*). The results for the deployment period over which all three instruments were operative are shown in Figure 4a along with ozone data at the two sites in Figure 4b. The detection limit of the DOAS was relatively high during these experiments due to the modest beam path, and the DOAS data below the dynamically computed LOD (taken as twice the computed error) were not plotted. Generally, it cannot be expected that over a distance of 12 km three very disparate techniques would produce very similar HCHO temporal profiles. The prevailing winds were generally from the southwest, especially at higher windspeeds, the mean value of which was relatively low during the study period. This made the CFA site downwind of the Polk Building site most of the time, especially during daylight hours, and contributed to the remarkable agreement between the three data sets. At nighttime, the CFA sampling location in the Cumberland River valley often lead to a decoupling of the air in and above the valley. Noting that the abscissa markings in Figure 4b correspond to midnight, it will be observed that while daytime ozone maxima in the two sites closely correspond to each other, there is often significant difference in nighttime/early morning hours. At nighttime, the stability of the atmosphere makes a comparison between the long-path DOAS and the TDLAS difficult due to insufficient mixing of the air. Consequently, it will be observed that for the DOAS data there is much better agreement in the daytime when the HCHO mixing ratios are also higher and the estimated errors in the DOAS data are less important (which spanned ±0.23 to ±1.64 ppb in the period shown). The HCHO data from the Polk Building site starts to be noticeably different beginning on the night of July 3 and continues through July 6. During this period, while the HCHO readings coincide during the daytime peaks, the important difference is that the regular diurnal pattern of the HCHO levels measured at this site until this point were disrupted—the morning lows measured at the Cornelia Fort site during these days were not observed at the Polk site. A local atmospheric perturbation rather than instrument malfunction is suggested by the return to agreement on July 7. The most plausible explanation of this is the Independence Day associated celebrations (Saturday July 3 through Monday July 5, constituting a long weekend) and reactive VOCs produced either from pyrotechnics or from vehicular traffic at night, remaining trapped in the urban island center and reacting in the morning. Heavy automobile traffic was associated with the night of July 4 and was directly viewable from the top of the Polk Building prior to the fireworks display and doubtless contributed to primary HCHO emissions. The fireworks were set off at the river within a short distance from the Polk Building. The rise in HCHO coincided with the high level of traffic coming into the area. Regrettably, VOC data were not available for this weekend; however, it may be noted that the last 5 canister samples before the weekend collected at 3, 5, 7, and 10 p.m. on June 27 and at 1 a.m. on June 28, respectively, measured a total of 54, 172, 85, 94, and 55 ppb C for 164 different compounds, whereas a similar sample collected at 7 a.m. on July 6 measured 495 ppb C. The micrometeorology around the Polk Building site can lead to unusual conditions; it is known that there can be significant photochemical activity in the immediate vicinity of the site, especially under stagnant conditions, and unusually high trace gas concentrations have been measured by others at this site (*60*, *73*). It is noted in Figure 4b that ozone levels on July 5 and 6 were the highest during the study period, substantially higher than the corresponding Monday/Tuesday values the previous week. It would appear that the trapping of emissions in an urban canyon can affect the observed chemistry in a given area for several days.

Atlanta. An overview of the 1999 Atlanta Supersite Study is available elsewhere (*74*). The measurement of HCHO and many other trace gases at this site was occasionally impacted by primary emission sources very close to the sampling site.

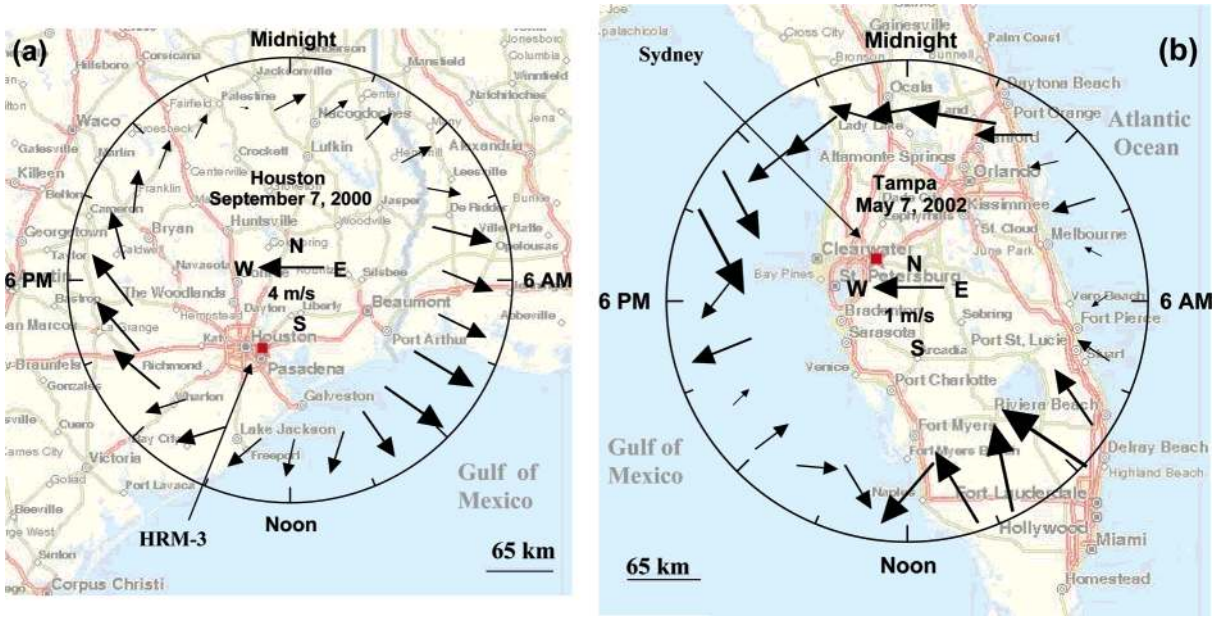

FIGURE 3. Diurnal land−sea breeze circulatory pattern aids the removal of accumulated pollutants. A very systematic pattern of change of wind direction at the Houston HRM-3 site is shown in panel (a); more often, the overall change in direction occurs in a 24 h period but not in so regular a fashion, as shown for Tampa in (b). The size magnitude of the arrows indicates the wind speed; the wind direction is indicated by the direction of the arrow. In both panels the background shows the sampling location (red star) in a 550 km × 550 km map.

Figure 5 shows the data for a number of trace gases for a 48-h period beginning at midnight August 12 . At this site, HCHO typically reached the peak concentration by 11 a.m.−noon, the 18 ppb peak observed on August 12 was the highest during this study but comparable concentrations were observed at other times. That this is at least partly due to atmospheric oxidation reactions is strongly suggested by the accompanying HNO_3 peak. See also similar behavior on August 13. Peak ozone mixing ratios on August 12 exceeded 175 ppb. Relative to HCHO, both O_3 and H_2O_2 reach maximum concentrations much later in the day. Photolytic removal of HCHO leads to an earlier maximum. The unusual midnight excursion of NO_2 and HCHO (occurring very late on August 12) was observed several times at this site. This is not accompanied by other oxidants or •OH reaction products such as HNO_3. However, the large CO peak accompanying this event strongly suggests an automotive source and indeed on this stagnant night (average windspeed from 10 p.m. to 2 a.m. was <1 m/s) there was a street racing event in the immediate vicinity of the site. Methanol and nitromethane are commonly used as fuel modifiers to boost power in engines modified for racing.[75] We were unable to find exhaust characteristics for nitromethane but it is likely to produce exhaust enriched in both NO_2 and HCHO, whereas methanol is known to produce large amounts of HCHO.

Houston. The measurements in Houston were carried out as part of TEXAQS 2000. Peak HCHO concentrations measured in Houston were much higher than those in other cities. On 7 out of 35 days of the study period, the daily HCHO maxima exceeded 25 ppb. HCHO formation during TEXAQS 2000 was previously examined from an airborne platform (*25*). Highest concentrations were observed at low altitudes, indicating surface precursors for HCHO; the maximum HCHO mixing ratio measured was 32 ppb at ~600 m. The highest levels of HCHO precursors and VOC reactivity were measured in plumes from petrochemical facilities that were concentrated around the Houston ship channel. Both HCHO and O_3 production was greatly enhanced in these plumes relative to power plant or mobile source emission plumes. Excellent linear correlations of NO_y and O_3 were observed in these plumes. The observed production of high levels of HCHO (>30 ppb) and O_3 (200 ppb) was accurately modeled using •OH-initiated chemistry with just ethene and propene, the inferred emissions being far greater than inventory reports (*25*).

Our ground-based observations were in remarkable accord with those of Wert et al. (*25*). On all days when the HCHO mixing ratio exceeded 25 ppb, short-term air mass back trajectories indicated that the air parcel arrived at the HRM-3 site from the ship channel. Figure 6 shows the wind rose over the study period with the center of the rose at the HRM-3 measurement site. The site is impacted by one or the other portion of the ship channel when the wind direction ranges from 45° to 145°. The mouth of the channel is in the 130°−135° direction. The La Porte airport is indicated by an arrow in Figure 6, in the 135° direction, 24 km from HRM-3. During TEXAQS 2000, the La Porte Airport was the most heavily instrumented site, with HCHO measurements made at this site by the UCLA DOAS. Figure 7 shows the La Porte vs the HRM-3 measurements. The DOAS ME beam path was 475 m long at a height of 2 m; the WT beam path, 1.9 km long, ranged from a height of 2 m to 44 m. The temporal patterns at the two sites are qualitatively very similar. Because the peak concentrations are generally produced with the prevailing wind direction from the mouth of the channel, the La Porte site registers the peak levels slightly before HRM-3 most of the time and generally at higher concentrations. Within the constraints of the atmospheric lifetime of HCHO on a typical sunny day, and the transport time between the sites (given the typical windspeed, see Figures 6 and 8) this agreement is remarkable, and it is tempting to conclude that the plumes originating from the ship channel may not be as spatially limited at the ground level as suggested by the aircraft experiments (*25*). However, there are both primary sources of HCHO and reactive VOC sources between La Porte and HRM-3, and even given the appropriate transport vector, whatever is observed at La Porte must be modified by direct emission, photochemical formation, and photolytic loss processes before the same air mass is observed at HRM-3. Nevertheless, given the appropriate wind vector, it appears that these plumes would be perceptible at Aldine, NW of HRM-3, and likely beyond Beltway 8.

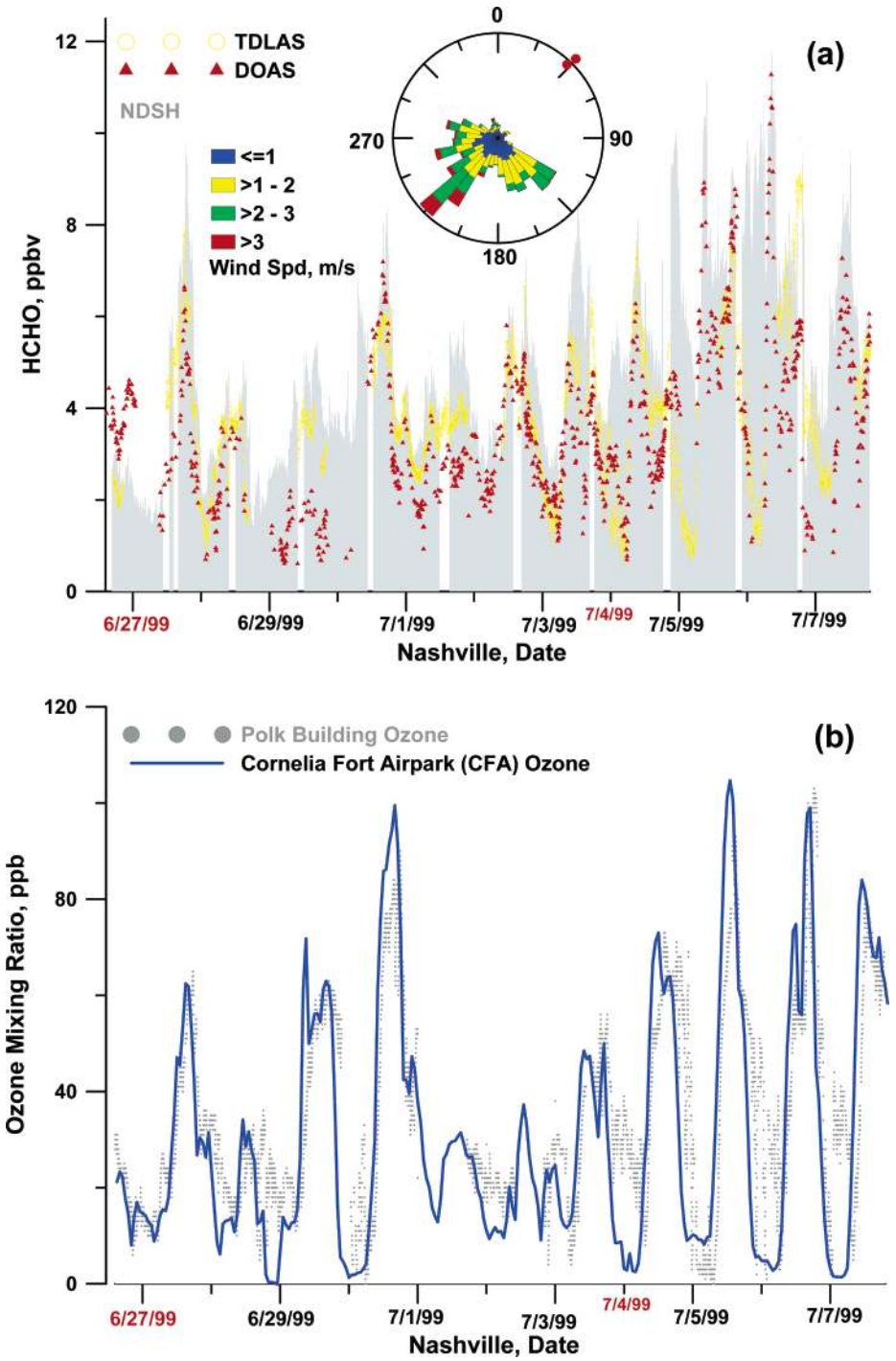

FIGURE 4. (a) HCHO data from three different instruments in Nashville. The inset shows the wind rose (wind direction is to the center of the rose, which is the location of the Polk Building) over the study period. The Cornelia Fort location where the TDLAS and the meteorological station were located is the inside red dot near the circumference. The path between this and the outer red dot constitutes the DOAS beam path. The top contour of the shaded data are from the NDSH instrument at the Polk Building, the gaps in the data that appear as white vertical bars indicate instrument calibration/maintenance periods. (b) Ozone mixing ratios at the two different locations in Nashville. Sundays in both panels are indicated in red.

At HRM-3, a difference frequency generation (DFG) tunable laser spectrometer (*76*−*77*), collocated with the NDSH instrument, also measured HCHO from August 21 to 25. At levels >5 ppb HCHO, the instruments produced essentially superimposable response, but at levels ≤5 ppb, the noise in the DFG instrument data was generally too great to permit a meaningful comparison.

The air mass for the highest HCHO concentration observed at HRM-3 did not pass through La Porte. In addition to 24 h back trajectories (shown in the top inset), Figure 8 also shows hourly wind directions and windspeed with ±1 standard deviation indicated. Given the shortest distance of the channel from the receptor site (marked with an *), and the prevailing wind speed, the air mass leading to the peak HCHO concentration originated at the channel ∼2 h before it arrived at HRM-3. The map also shows the location of La Porte and the ship channel. There are no major primary emission sources of HCHO between the nearest point in the ship channel and HRM-3. During the entire 3 h preceding the peak HCHO concentration at 14:30, the wind was from

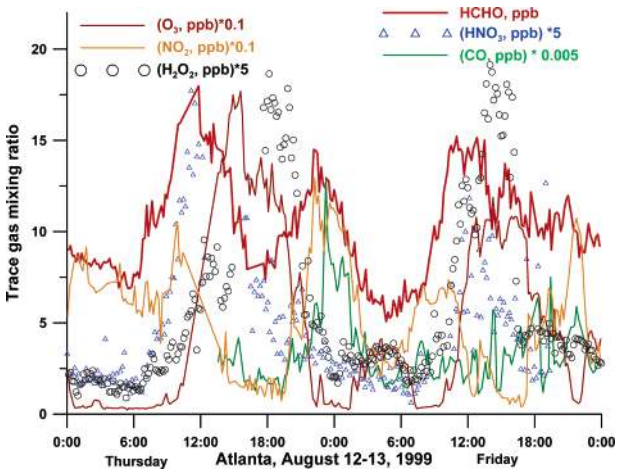

FIGURE 5. HCHO, HNO_3, CO, O_3, NO_2, and H_2O_2 mixing ratios over a 2-day period in Atlanta. See text for details.

due East, the nearest channel location. One further infers that the emission of the precursor (such as ethene or propene) which leads to the atmospheric formation of formaldehyde must have taken place as a pulse rather than as a continuous release. Otherwise, based on the stability of the windfield and that of the insolation intensity (not shown) during the entire period, the resulting HCHO pulse would have been much longer in duration.

Referring to Figure 6, the other dominant wind directions were from ~190° and 55°. The HCHO concentration was relatively low when the air mass originated from these directions. Figure 9 shows the HCHO concentration measured from September 17−19 and the 24-h back trajectories for September 16−19. On September 16 and 17, the air mass came from the northeast, originating in northern Louisiana and coming through the least industrialized parts of Houston. By Houston standards, the HCHO mixing ratio remained very low: the maxima during these 2 days was <10 ppb. But on 9/18, the wind direction changed from NE to SE, and the air mass came directly through the ship channel, there was a large increase of HCHO mixing ratio, reaching ~40 ppb at ~11:30 a.m. on 9/18. On 9/18, there was also an unusual ~15 ppb midnight HCHO peak. Analysis of wind direction data strongly suggests that this unusual peak relates also to wind direction change. From 6 p.m. 9/17 to 4 a.m. 9/18, the wind direction rotated through nearly 360°. There is a small nitric acid excursion during this period but it is generally smaller in proportion to HCHO (relative to the daytime peaks on 9/18 and 9/19). However, in marked contrast to the situation with the occurrence of the daytime peaks, ozone was titrated to a zero concentration by very large NO emissions that occurred simultaneously with the HCHO peak with maximum NO concentrations registering just before and after the HCHO peak. The HNO_3 excursion coincides with the second NO peak. The source of the NO emission is most likely industrial flaring; it is routine practice in the petrochemical industry to carry out nocturnal flaring. We surmise that the nocturnal HCHO peak resulted from simultaneous reactive hydrocarbon emissions from the same or a separate source and reaction with flame-generated radicals or flame-induced reactions. Note that other emissions of NO, e.g., during the early morning hours of 9/18 and 9/19, are not accompanied by HCHO peaks. On 9/18, the air parcel came directly through the shipping channel; on 9/19, it just skirted the channel. It is interesting to note that the large daytime HCHO peaks on 9/18 and 9/19 are strongly correlated with ozone and HNO_3, suggesting •OH-driven chemistry. There is also strong correlation of these peaks with SO_2 levels suggesting the emission of the VOCs responsible for HCHO formation is tied to the observed levels of SO_2. Space precludes a detailed analysis here but we also measured the rate of particulate sulfate formation. The rate of sulfate and HNO_3 production during the ascending portion of the HCHO excursion on 9/18 is linearly correlated with the rate of HCHO production (linear $r^2 > 0.95$). In addition, the measured H_2O_2 levels (not shown here) correlate *positively* with the SO_2 emissions, suggesting a relatively fresh plume and a common source for the SO_2 and peroxy radical generation. All of these strongly suggest •OH-driven chemistry. It is worthwhile noting that ozone maxima at the HRM-3 site were frequently observed relatively early in the day, often before noon, as it appears in Figure 9. The ozone maxima in such cases do not coincide with the maximum in the insolation intensity but are controlled by the VOC emissions.

Philadelphia. Although peak HCHO levels were modest compared to some of the other sites, there were 4 episodes during the 34 day measurement period. In the last 4 days of June, the daily maxima ranged from 7.5 to 8 ppb, a relatively high level for this study. Back trajectories indicated that on 3 of the 4 days, the air mass arrived from the downtown area, 13 km SW of the site. The other three episodes happened during July 9−10, July 16−17, and July 22−25. In all these episodes, the air parcels arrived from the northeast. Both Trenton (~20 miles) and New York City (~100 miles) are located in this direction; however, given the atmospheric lifetime of HCHO, Trenton, or the industrialized corridor leading to it, is the likely origin.

Figure 10 shows HCHO concentrations along with those of H_2O_2, methyl hydroperoxide (MHP), HNO_3, O_3, NO, and SO_2 for 9 days beginning July 9. The HCHO excursions for this period began shortly before midnight on 7/9 and started abating on the morning of 7/10. Aside from its nocturnal occurrence, there is other evidence that this is a transported polluted air mass. The H_2O_2 value is low as can be expected at nighttime. There is a small excursion in HNO_3 that occurs exactly between the two HCHO peaks; a significant peak in HNO_3 is seen only around 7/10 noon when the major HCHO excursion is essentially over. The observed HCHO did not, therefore, originate from local •OH-driven chemistry. Completely coincident with the major nocturnal HCHO peak, there are peaks in SO_2 and NO. Not shown is an excursion in particulate sulfate that starts at the same time as the SO_2 peak on the morning of 7/10 but does not reach the maximum ($>17\ \mu g\ m^{-3}$) until late in the afternoon as the SO_2 is converted to sulfate. The NO levels are high enough to completely titrate the ozone. It is possible that the NO excursion is from a more local emission, as there are even greater NO excursions in the midnight to early morning hours several times in the period shown in Figure 10 (and for the rest of the study not shown in this figure), irrespective of the direction from which the air mass arrived. One of the more interesting aspects of the 7/9−7/11 period is the persistent presence of relatively high mixing ratios of MHP (0.5−1 ppb) not observed at any other period during the study—we are unable at this time to elucidate the chemistry that led to the formation of MHP. However, we note that during this period and this period only, MHP and H_2O_2 concentrations were very poorly correlated.

From 7/11 to 7/15, the wind came largely from the southeast and the east. The concentrations of HCHO and most of the other species shown were modest, other than the nocturnal NO emissions. The wind direction began to shift late on 7/15. On 7/16 and 7/17, the wind direction was persistently from the northeast. As evidenced from the >30 ppb SO_2 peak, a plume arrived on the morning of 7/17 (late in the afternoon of 7/17, particulate sulfate reached ~31 $\mu g/m^3$, the highest value during this study). On the basis of the close correspondence with the HNO_3 formation, the HCHO

FIGURE 6. Windrose, Houston, TX, TEXAQS 2000 study period with the wind blowing to the center of the rose where the HRM-3 site is located. Note that one of the dominant wind vectors comes from the direction of La Porte, the location of the UCLA DOAS.

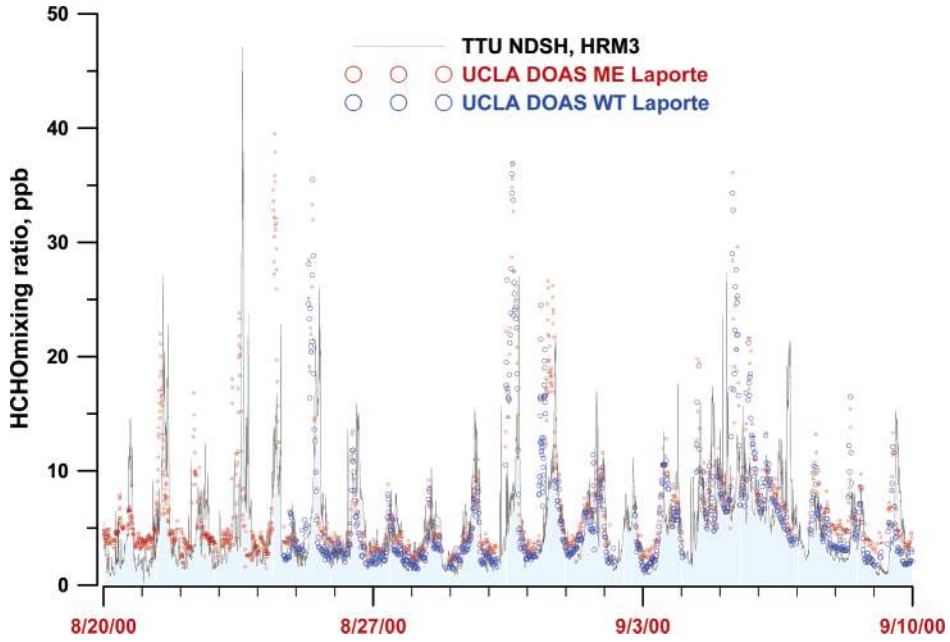

FIGURE 7. HCHO mixing ratio measured at HRM-3 by the NDSH instrument vs HCHO mixing ratios measured in La Porte by the UCLA DOAS with two different beam paths. The tic marks correspond to midnight. The ME beam path is 475 m at 2 m height; the WT beam path is 1.9 km at an average height of 23 m. Sundays are marked in red in the abscissa labels.

peak in this case, unlike the episode discussed earlier, would appear to originate from local •OH-driven chemistry.

Bay Region Atmospheric Chemistry Experiment (BRACE, 2002, Tampa, FL). In Tampa, the daily peaks of HCHO occurred almost exactly at the same time each day, shortly before 3 p.m. The ozone concentration peaked almost without exception at the same time as well. Neither this synchrony nor this specific timing was observed in such a regular manner in any of the other cities. The composite diurnal profile of HCHO over the study period as shown in Figure 1e underscores an extremely regular pattern observed at this site. The absolute intensity of the afternoon peak during any weekday was observed to be dependent primarily on the wind direction in the early afternoon hours—if the wind was from the downtown area, the HCHO concentration increased. For the first ~3 weeks of the study, through 5/17, there was no precipitation. The afternoon wind directions ranged from 220±80° (the city center was at 270°), and relative to the latter period of the study, the HCHO maxima were higher (see Figure 1e), reaching the study maximum of 9 ppb on 4/30 when the wind was exactly from 270° all afternoon. It rained consecutively on 5/18 and 5/19. From 5/19 to 5/28, the wind direction shifted to 80 ± 60° and the diurnal HCHO maxima remained <4 ppb. During the last 3 days of the month, the prevailing wind direction changed again to 290 ± 30° with an accompanying rise in the HCHO maxima.

The highest HCHO mixing ratio (16 ppb) during the study was observed on an aircraft flight late in the afternoon of May 13 while following the urban plume ~50 km SE of downtown Tampa at a low altitude (175 m). In general, HCHO concentration decreased with altitude: this is discussed in more detail later. The second highest mixing ratio (12.4 ppb)

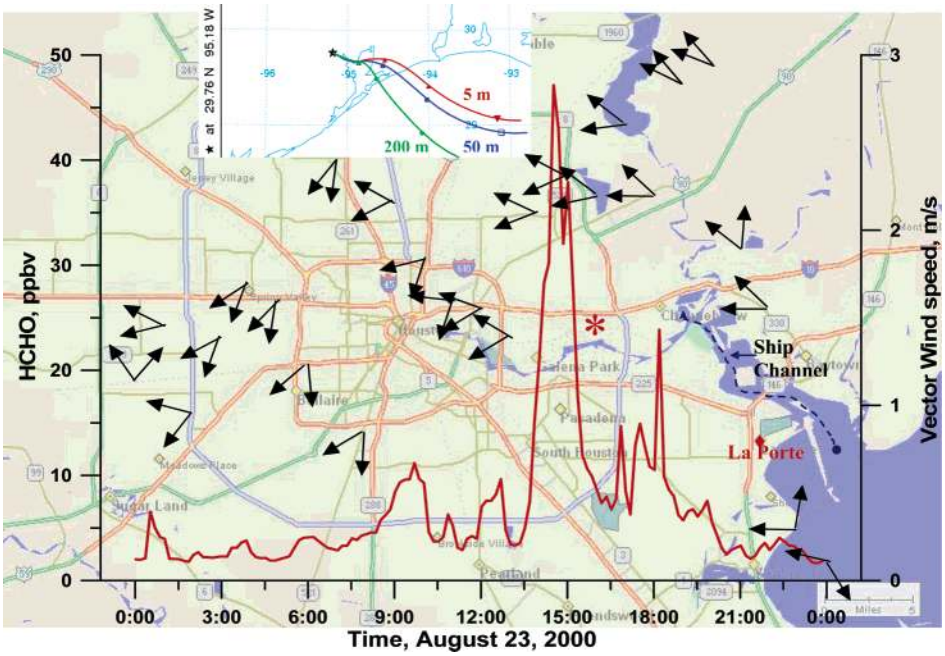

FIGURE 8. Map of the measurement location is shown in the background, with the HRM-3 measurement site indicated by the red asterisk. The top inset shows 24 h back trajectories ending at the receptor site at 14:30 h (at the time the maximum HCHO mixing ratio was observed); the trajectories at all three heights come directly through the ship channel area. (The trajectories here and in Figure 9 were obtained by the NOAA HYSPLIT model, courtesy of NOAA). The HCHO mixing ratio is the deep red trace (left ordinate). The evolution of the windfield is depicted by pairs of arrows that encompass ±1 standard deviation in wind direction over that hour and the vertical position indicates the vector wind speed (right ordinate).

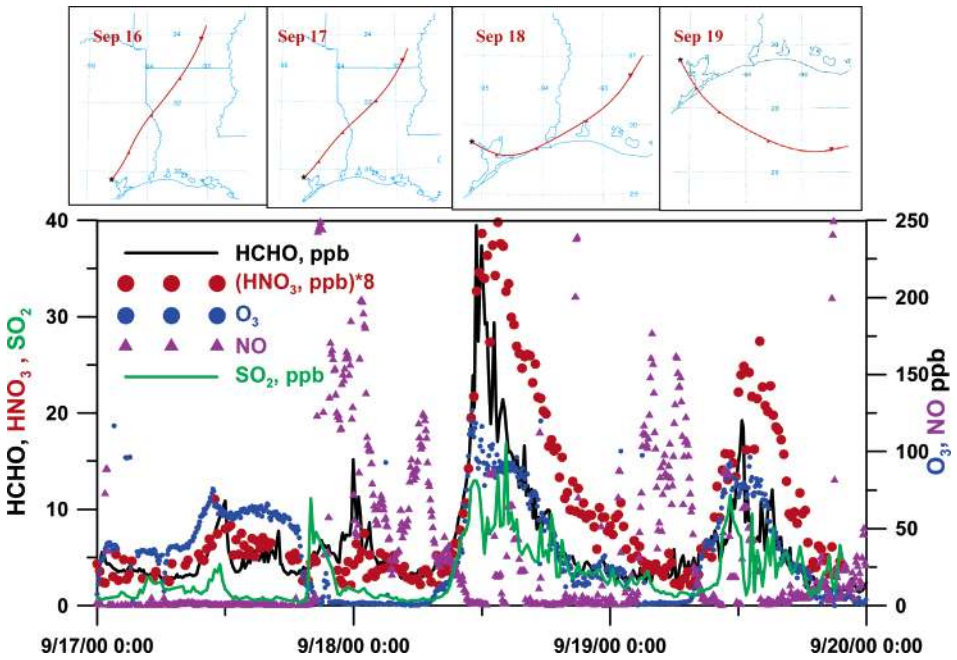

FIGURE 9. Mixing ratios of trace gases, HRM-3, Houston 9/17/00−9/19/00. The 24 h backward trajectories for 9/16/00−9/19/00 are shown on the top.

was observed on another flight on May 30 just south of St. Petersburg, also late in the afternoon and at a relatively low altitude (350 m). We discuss here one of the more typical of the >20 flights from the BRACE campaign, conducted on May 8, 2002. On this date, southeasterly flow in the morning was expected to push the Tampa/St. Petersburg plume over the Gulf, while the onset of westerly flows in the afternoon was expected to push the aged air mass ashore north of Tampa. The flight plan was therefore designed to capture the effects of land−sea breeze circulation. Refer to Figures 11 and 12 for the following description. The aircraft took off at 2:25 p.m. and executed a spiral ascent to ~3 km over the ground site in Sydney (location 1 in Figures 11 and 12; hereinafter the locations are noted by the parenthetical numerals). Note the abrupt decrease in HCHO and O_3 concentrations upon leaving the well-mixed boundary layer. The aircraft then proceeded at this altitude SW to a point just offshore (2), descended to 60 m (note the increase in HCHO concentration upon descent), and proceeded over water first N to (3), then NNW to (4), then NW to a point ~10 km W of Bellaire Beach (5), then heading NNE to maintain a course parallel to the coast line, maintaining approximately the same

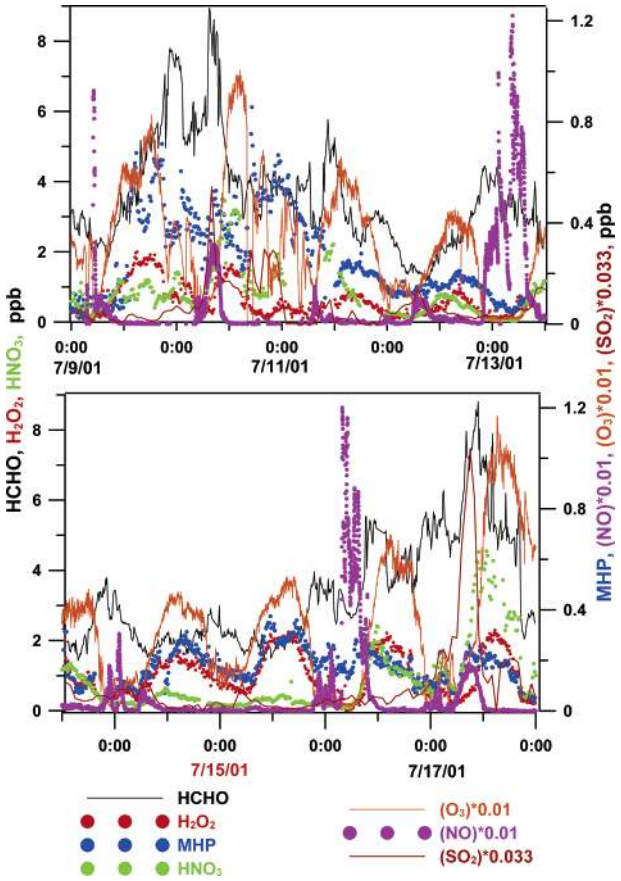

FIGURE 10. Trace gas mixing ratios over a 10-day period in Philadelphia, PA. Sunday is marked in red.

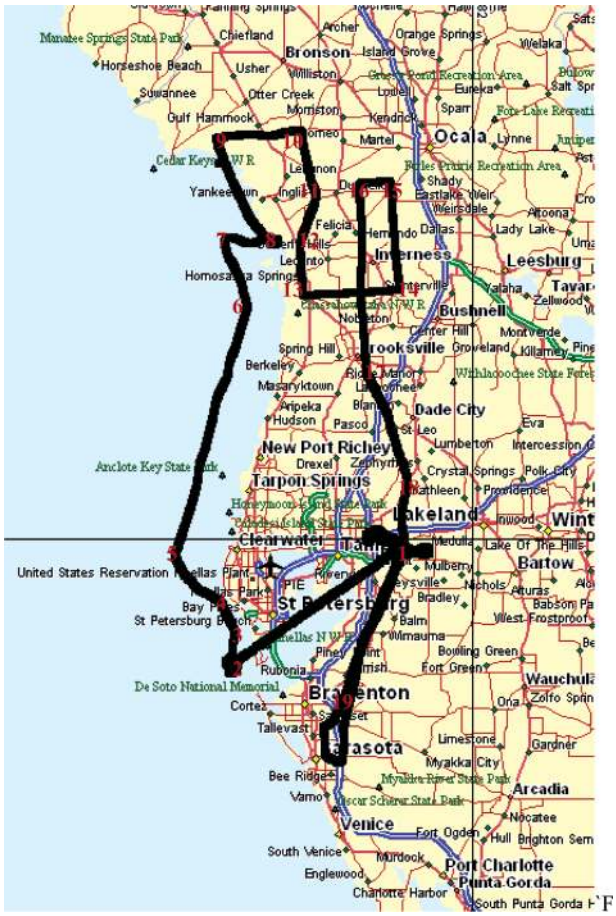

FIGURE 11. Flight path of the NOAA Twin Otter, Wednesday, May 8, 2002, South Florida.

distance from the coast to a point parallel to Chassahowitzka (6), veering NNW to a point W of the Crystal River power plant (CRPP, 7), turning E and ascending to 150 m before landfall (8). At this point, the aircraft encountered the tail end of the polluted air mass as it was advected eastward. Note the abrupt rise in O_3, condensation nuclei (CN) count, HCHO, and most strikingly HNO_3. There is minor and scattered increase in SO_2 concentration, but also, importantly, the H_2O_2 level decreases abruptly. The flight headed NNE to define the edge of this polluted air mass while hugging the coastline until land was reached near Cedar Key (9). By this time, this initial peak in HNO_3 has decreased to half the peak value (in other flights in this series, rapid loss of HNO_3 via reaction with sea salt aerosol was seen, see reference *78*); H_2O_2 has also recovered about halfway (that aqueous phase H_2O_2−S(IV) reactions had little to do with the H_2O_2 levels is evident from the persistent presence of SO_2 at about the same level), and ozone has returned also almost to the pre-excursion level. As the aircraft headed E to proceed inland, a zone of elevated HCHO was encountered, with HNO_3 and O_3 also showing minor peaks accompanied by a small but discernible depression of H_2O_2. As the aircraft proceeded further E for 22 km to (10), halfway through this transit HCHO began increasing, while HNO_3 decreased and O_3 remained stable. Concomitantly, H_2O_2 showed a small peak as the HCHO plateau concentration was reached, indicating a relatively aged polluted air mass where photochemical processing has largely been completed. At (10), the aircraft headed S to proceed to a point W of Inglis (11); with the exception of a minor peak (accompanied by a depression in H_2O_2), HCHO mixing ratio remained stable at ~7.8 ppb. As the aircraft turned SSW toward (12), it traversed a plume that would appear to be from a nearby point source (because of the high concentrations and sharp spatiotemporal definition), reaching a CN count of 20 000 per cm^3, and SO_2, NO_2, and NO (not plotted) peak mixing ratios of 140, 32, and 11 ppb, respectively. On the basis of the locale and the back trajectory of the air mass, this plume was likely from the CRPP, the largest point source of NO_x (39 400 Mtons/yr) and SO_2 (103 500 Mtons/yr) in Florida. Titrated by the NO, the O_3 mixing ratio decreased sharply from 70 to 35 ppb. This portion of the data is shown with an expanded abscissa scale in the right panel in Figure 12 for clarity. H_2O_2 concentration also decreased; it is likely that the decrease would have been much more noticeable with a faster instrument response time. There was likely liquid water in the plume and the aqueous phase H_2O_2−S(IV) reaction is at least partly responsible for the disappearance of H_2O_2. On the basis of the observed chemistry, the HNO_3 concentration reached a minimum correspondent to the ozone minimum. But following this, the levels rose. This HNO_3 may have been formed in the plume itself or it can be an instrument artifact at the high NO_x levels: the converter difference technique is capable of providing fast response but high background NO_x levels, of course, make it difficult to measure low levels of HNO_3 accurately. As the aircraft proceeded to the S end of this leg to a point near Homosassa (13), the HCHO concentration reached a minimum completely coincident with the local H_2O_2 maximum. Then HCHO and O_3 levels began to rise again as NO levels returned to pre-plume, negligible values. The aircraft turned E again for 28 km to reach (14), at which point O_3 recovered to the pre-plume value and both HCHO and H_2O_2 reached values slightly higher than their pre-plume values. As the aircraft turned N again toward (15), both O_3 and HCHO levels rose again but HNO_3 values remained stable. The O_3 peaked after HCHO and reached a maximum at (15): this situation likely arose from

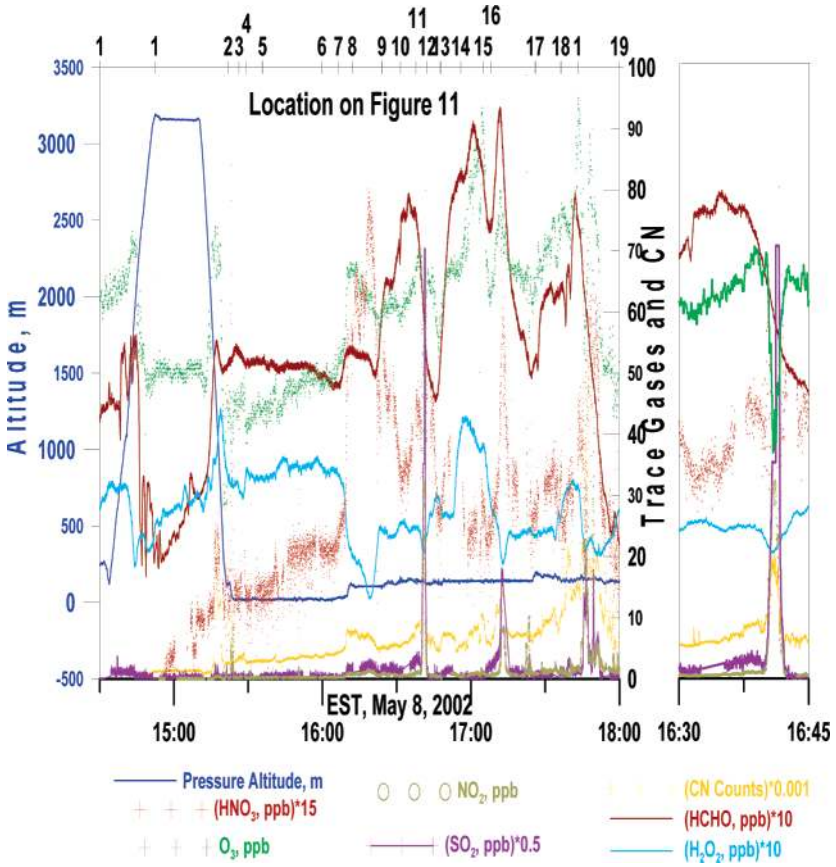

FIGURE 12. Selected parameters measured during the flight depicted in Figure 11. The flight coordinates (Alt., Lat., Long.; the blue line, gray short and long dashed lines, respectively) all refer to the left ordinate; only the terminal axis values are shown for latitude and longitude. All trace gas and condensation nuclei counts refer to the right ordinate. The numeric designations on the top abscissa refer to numbered locations on the flight track in Figure 11. The right panel shows an expanded view of the brief period covering the plume traverse.

olefin oxidation chemistry as seen in Houston. An increase in HNO_3 was not observed because NO_2 was virtually absent. While we have no conclusive proof that olefin oxidation is involved, a total of 11 canister samples were taken at irregular intervals during this flight. The sample taken several minutes after this point showed the highest olefin mixing ratio: 4.4 ppb vs an average of 2.3 ppb for the rest of the flight. In any case, differing wind fields, humidity, and CO levels (not shown here) on the flight track from 14 to 15 demonstrate that this is a separate air mass from the CRPP plume. At the end of this traverse, the aircraft turned upwind W for 9 km toward (16). At this time, we do not understand the highly coincident decreases in O_3 and HCHO concentrations that occurred as the aircraft reached (16). The aircraft then turned S toward Brooksville (17), and shortly afterward encountered a plume for the second time (quite likely the same plume encountered between (11) and (12), as the air mass was moving W), though more dispersed. That this plume is aged relative to the first encounter is indicated by the lack of NO (~1 ppb) and the rapid rise in O_3, HNO_3, and HCHO accompanying the peaks in SO_2, NO_2, and CN, and a pronounced decrease in H_2O_2. By the time the aircraft reached (17), it encountered another modest plume, (4 ppb SO_2, 10 ppb NO_2, 2 ppb NO) with O_3 and HCHO both reaching individual minima while H_2O_2 remained at a stable low value. As the aircraft headed SSW to Zephyr Hills (18), HCHO rose to a stable plateau value. All of the gases except H_2O_2 reached another set of peak values as the aircraft traveled S to Sydney (1), where it likely encountered the Tampa urban plume. HCHO concentrations decreased monotonically as the aircraft traveled further SSE to Bradenton and Sarasota (19). At the S end of this track, the aircraft turned N, ascended to 460 m and then descended to land at 6:32 p.m.

Vertical Profile of Formaldehyde Around Tampa. A number of past aircraft-based HCHO measurements have established that HCHO concentrations decrease monotonically with altitude (*29*, *32*, *40*, *79*−*81*) However, all of these studies pertain to remote regions, especially over the ocean, and extend to altitudes up to 12 km. Altitude profiles of formaldehyde in or around an urban area, extending to low altitudes, have never been reported, and, as shown below, provide a more variegated picture than over the remote open ocean. Because of the proximity of the Gulf of Mexico, Tampa provides a unique location to measure such profiles both over land and over the Gulf. The decrease in concentration with altitude was observed also in the majority of the flights here, often in a monotonic fashion with a steep slope as shown in Figure 13a, reaching near-zero levels at the top of the ascent. Figure 13b shows three ascent and descent profiles which show that the rate of decrease with altitude can be steep to modest to near zero. Figure 14 shows the altitude profiles from experiments from various flights in which the height of the boundary layer (BL), as determined from on-flight measurement of meteorological parameters, is also shown. It should be recognized that the demarcation of the boundary layer is often diffuse rather than abrupt and certainly much broader than the width of the vertical lines in the figure might indicate. Low-altitude HCHO mixing ratios were not necessarily lower over the ocean: in the data presented, the highest HCHO mixing ratio at low altitudes is seen in sample 7 (Figure 14), when the urban plume was advected over the Gulf. All of the measurements shown were

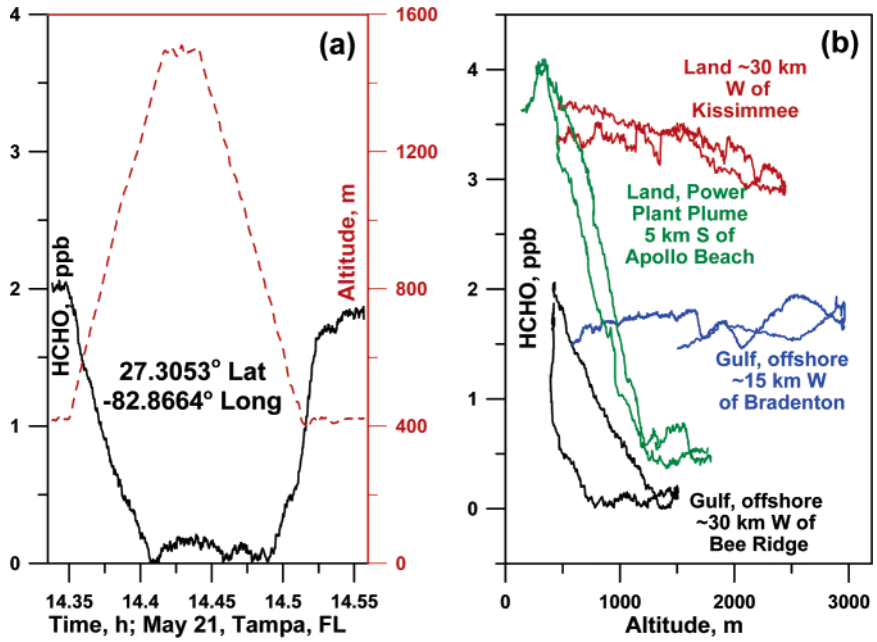

FIGURE 13. (a) Decrease in the mixing ratio of HCHO with altitude is readily observed in the trough and hat patterns during successive ascent and descent over the Gulf, (b) vertical HCHO profiles over both land and the sea in a series of spiral up/down experiments near Tampa, FL.

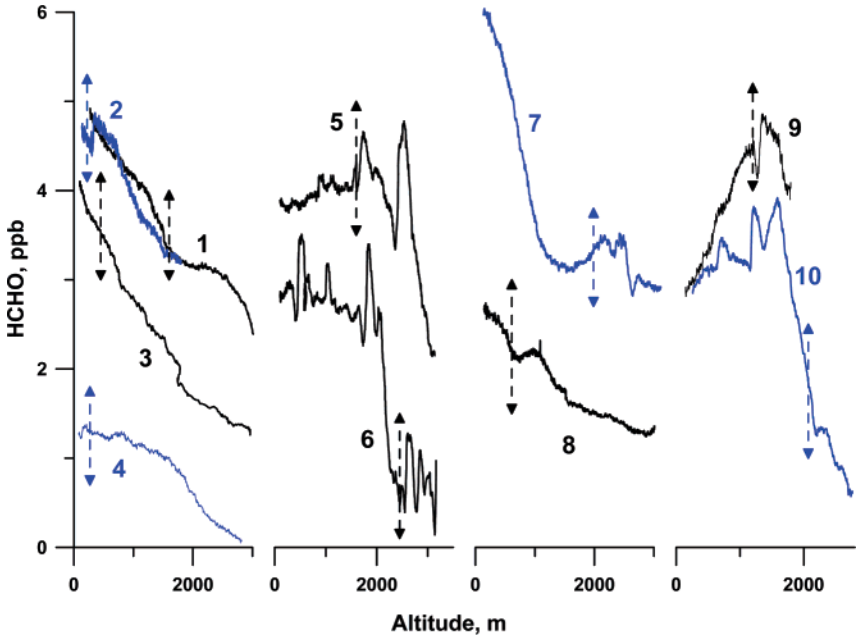

FIGURE 14. Illustrative altitude profiles of HCHO over land (black) and water (blue trace) near Tampa, FL. Points 1, 3, 5, and 6, profiles over Sydney, FL (ground measurement site) on different days; 2, over Gandy Bridge in Old Tampa bay; 4, over the Gulf, 35 km N of Largo; 7, over the Gulf, 15 km SW of St. Petersburg; 8, 6 km W of St. Petersburg; 9, near shore, 8 km SW of Apollo Beach; and 10, over the Gulf, 50 km W of Osprey. The approximate location of the boundary layer is indicated by double-ended vertical arrows.

made between 2:00 and 3:30 p.m. EST, the window within which highest HCHO mixing ratios generally occurred in Tampa, except for 3 and 10, which were carried out just before noon and just after 7 p.m., respectively. In the latter case, the aircraft followed the urban plume out over the Gulf as evening descended. It will be noted that 1, 3, 5, and 6 represent profiles over the same location: the ground chemistry supersite at Sydney. Flights 1 and 3 represent very similar meteorological conditions except earlier and later in the same day; in the latter case, the HCHO level starts lower and decreases monotonically through a relatively low BL,while in the former case the HCHO levels becomes constant around the BL, before dropping again; this latter pattern is quite commonly observed, either over land (1, 8) or over the Gulf (4, 7, 10). Profiles 5 and 6, at the same location on different days, also have certain similarities, in that at low altitudes HCHO levels are relatively invariant and drop abruptly approximately just after or before the top of the BL is reached. Brief discontinuities just as the BL is reached (2, 9), are also observed: in both of these cases the top of the BL was sharply defined. Profiles 9 and 10 represent rather unique cases in this data set where the HCHO mixing ratio *increases* with altitude until approximately the top of the BL is reached; the concentration then drops abruptly. In both cases, NO_y profiles followed an identical pattern, suggesting a buoyant plume origin.

The monitoring results using NDSH instruments to measure ambient levels of HCHO on a semi-continuous basis have been shown in five cities. Agreement of this method with TDLAS and DOAS methods when sampling the same air masses indicates its viability as an inexpensive compact alternative. Analysis of HCHO results with concurrently collected data from other multiple urban locations confirm contributions from both primary sources such as automobiles and the photochemical origin of secondary HCHO. Formaldehyde is not efficiently washed out by precipitation at least in the present ground-based studies. Trapping of precursor emissions in urban canyons can lead to sustained photochemical production over several days. As with many other trace pollutants, meteorological circulation patterns can have a profound influence on the observed concentrations, especially in coastal cities. The decrease of HCHO mixing ratios with altitude, particularly above the boundary layer, takes place in urban areas, just as it has been reported to occur in remote maritime regions. The data set presented here can be used as a benchmark for future measurements if the use of formaldehyde precursors such as methanol or methyl *tert*-butyl ether as oxygenated fuel additives increase in the future. For ground-level measurements, a time resolution of 10 min, as practiced with the current NDSH instruments, seems to be adequate for the near future. However, the best time resolution of 2 min attainable with these instruments is not adequate for measurements from an aircraft. This response time needs to be improved by an order of magnitude to be attractive for aircraft use. Nevertheless, convenient, affordable measurement methods make it easier to generate data with greater spatial and temporal resolution, which allow better diagnostic testing of air quality simulation models. The latter then provide the basis for iterative improvement of the models; these results ultimately guide regulatory decisions.

Acknowledgments

This research was supported by the SOS/Supersite Research Program of the U.S. Environmental Protection Agency (USEPA); the Philadelphia field studies were supported by the USEPA through Man-Tech Environmental; the Bay Region Atmospheric Chemistry Experiment (BRACE) in Tampa, FL was supported in part by the Florida Department of Environmental Protection with the assistance of the Environmental Protection Commission of Hillsborough County. The preparation of this manuscript was partly supported by the U.S. EPA Science To Achieve Results (STAR) Program Grant RD-83107401-0. The United States Environmental Protection Agency through its Office of Research and Development collaborated in the research described here and partially funded portions under EPA Contract 68-D-00-206 to ManTech Environmental Technology, Inc. It has been subjected to Agency review and approved for publication. We thank L. T. Kleinman and K. J. Olszyna for auxiliary data from Nashville and E. B. Cowling for his help. J. Rice and Paul Klutz are thanked for help during the Nashville study. W. Crow and C. R. Philbrick are thanked for access to auxiliary data from Houston and Philadelphia.

Literature Cited

(1) Carlier, P.; Hannachi, H.; Mouvier, G. The chemistry of carbonyl-compounds in the atmosphere − A review. *Atmos. Environ.* **1986**, *20*, 2079−2099.

(2) Matthews, T. G.; Howell, T. C. Visual colorimetric formaldehyde screening analysis for indoor air. *J. Air Pollut. Control Assoc.* **1981**, *31*, 1181−1184.

(3) Lipari, F.; Dasch, J. M.; Scruggs, W. F. Aldehyde emissions from wood-burning fireplaces. *Environ. Sci. Technol.* **1984**, *18*, 326−330.

(4) Lee, M.; Heikes, B. G.; Jacob, D. J. Hydrogen peroxide, organic hydroperoxide, and formaldehyde as primary pollutants from biomass burning. *J. Geophys. Res.* **1997**, *102*, 1301−1309.

(5) Lee, M.; Heikes, B. G.; Jacob, D. J. Enhancements of hydroperoxides and formaldehyde in biomass burning impacted air and their effect on atmospheric oxidant cycles. *J. Geophys. Res.* **1998**, *103*, 13201−13212.

(6) Yokelson, R. J.; Goode, J. G.; Hao, W. M. Emissions of formaldehyde, acetic acid, methanol, and other trace gases from biomass fires in North Carolina measured by airborne Fourier transform infrared spectroscopy. *J. Geophys. Res.* **1999**, *104*, 30109−30125.

(7) Anderson, L. G.; Lanning, J. A.; Barrell, R.; Miyagishima, J.; Jones, R. H.; Wolfe, P. Sources and sinks of formaldehyde and acetaldehyde: An analysis of Denver's ambient concentration data. *Atmos. Environ.* **1996**, *30*, 2113−2123.

(8) Wagner, T.; Wyszynski, M. L. Aldehydes and ketones in engine exhaust emissions − A review. *Proc. Inst. Mech. Eng., Part D: J. Auto Eng.* **1996**, *210*, 109−122.

(9) Mitchell, C. E.; Olsen, D. B. Formaldehyde formation in large bore natural gas engines. Part 1: Formation mechanisms. *J. Eng. Gas Turb. Power* **2000**, *122*, 603−610.

(10) Alzueta, M. U.; Glarborg, P. Formation and destruction of CH_2O in the exhaust system of a gas engine. *Environ. Sci. Technol.* **2003**, *37*, 4512−4516.

(11) Olsen, D. B.; Mitchell, C. E. Formaldehyde formation in large bore engines. Part 2: Factors affecting measured CH_2O. *J. Eng. Gas Turb. Power* **2000**, *122*, 611−616.

(12) Liang, K. Y.; Pope, R. J. Case study: formaldehyde emissions from IC engines combusting digester gas using FTIR. *Proc. Air Waste Mgmt. Assoc.* **2002**, 3213−3223.

(13) Childers, C. L.; Huang, H. L.; Korzeniewski, C. Formaldehyde yields from methanol electrochemical oxidation on carbon-supported platinum catalysts. *Langmuir* **1999**, *15*, 786−789.

(14) Jusys, Z.; Kaiser, J.; Behm, R. J. Methanol electrooxidation over Pt/C fuel cell catalysts: Dependence of product yields on catalyst loading. *Langmuir* **2003**, *19*, 6759−6769.

(15) Mukund, R.; Kelly, T. J.; Spicer, C. W. Source attribution of ambient air toxic and other VOCs in Columbus, Ohio. *Atmos. Environ.* **1996**, *30*, 3457−3470.

(16) Li, S.-M.; Anlauf, K. G.; Wiebe, H. A.; Bottenheim, J. W. Estimating primary and secondary production of HCHO in eastern North America based on gas-phase measurements and principal component analysis. *Geophys. Res. Lett.* **1994**, *21*, 669−672.

(17) Lee, Y.-N.; Zhou, X.; Kleinman, L. I.; Nunnermaker, L. J.; Springston, S. R.; Daum, P. H.; Newman, L.; Keigley, W. G.; Holdren, M. W.; Spicer, C. W.; Young, V.; Fu, B.; Parrish, D. D.; Holloway, J.; Williams, J.; Roberts, J. M.; Ryerson, T. B.; Fehsenfeld, F. C. Atmospheric chemistry and distribution of formaldehyde and several multioxygenated carbonyl compounds during the 1995 Nashville Middle Tennessee Ozone Study. *J. Geophys. Res.* **1998**, *103*, 22449−22462.

(18) Palmer, P. I.; Jacob, D. J.; Fiore, A. M.; Martin, R. V.; Chance, K.; Kurosu, T. P. Mapping isoprene emissions over North America using formaldehyde column observations from space. *J. Geophys. Res.-Atmos.* **2003**, *108* (D6), Art. 4180.

(19) Chance, K.; Palmer, P. I.; Spurr, R. J. D.; Martin, R. V.; Kurosu, T. P.; Jacob, D. Satellite observations of formaldehyde over North America from GOME. J. *Geophys. Res. Lett.* **2000**, *27*, 3461−3464.

(20) Frost, G. J.; Fried, A.; Lee, Y. N.; Wert, B.; Henry, B.; Drummond, J. R.; Evans, M. J.; Fehsenfeld, F. C.; Goldan, P. D.; Holloway, J. S.; Hübler, G.; Jakoubek, R.; Jobson, B. T.; Knapp, K.; Kuster, W. C.; Roberts, J. M.; Rudolph, J.; Ryerson, T. B.; Stohl, A.; Stroud, C.; Sueper, D. T.; Trainer, M.; Williams, J. Comparisons of box model calculations and measurements of formaldehyde from the 1997 North Atlantic Regional Experiment. *J. Geophys. Res.* **2002**, *107* (D8), Art. 1029.

(21) Khare, P.; Kumar, N.; Kumari, K. M.; Srivastava, S. S. Atmospheric formic and acetic acids: An overview. *Rev. Geophys.* **1999**, *37*, 227−248.

(22) Dong, S.; Dasgupta, P. K. On the formaldehyde-bisulfite-hydroxymethanesulfonate equilibrium. *Atmos. Environ.* **1986**, *20*, 1635−1637.

(23) Lagrange, J.; Wenger, G., Lagrange, P. Kinetic study of HMSA formation and decomposition: Tropospheric relevance. *J. Chim. Phys. PCB* **1999**, *96*, 610−633.

(24) Zuo, Y. G. Light-induced formation of hydroxyl radicals in fog waters determined by an authentic fog constituent, hydroxymethanesulfonate. *Chemosphere* **2003**, *51*, 175−179.

(25) Wert, B. P.; Trainer, M.; Fried, A.; Ryerson, T. B.; Henry, B.; Potter, W.; Angevine, W. M.; Atlas, E.; Donnelly, S. G.; Fehsenfeld, F. C.; Frost, G. J.; Goldan, P. D.; Hansel, A.; Holloway, J. S.; Hubler, G.; Kuster, W. C.; Nicks, D. K., Jr.; Neuman, J. A.; Parrish, D. D.; Schauffler, S.; Stutz, J.; Sueper, D. T.; Wiedinmyer, C.;

Wisthaler, A. Signatures of terminal alkene oxidation in airborne formaldehyde measurements during TexAQS 2000. *J. Geophys. Res.* **2003**, *108*, Art. 4104.
(26) Lawson, D. R.; Biermann, H. W.; Tuazon, E. C.; Winer, A. M.; Mackay, G. I.; Schiff, H. I.; Kok, G. L.; Dasgupta, P. K.; Fung, K. Formaldehyde measurement methods evaluation and ambient concentrations during the carbonaceous species methods comparison study. *Aerosol Sci. Technol.* **1990**, *12*, 64−76.
(27) Alicke, B.; U. Platt; Stutz, J. Impact of nitrous acid photolysis on the total hydroxyl radical budget during the limitation of Oxidant Production/Pianura Padana Produzione di Ozono study in Milan. *J. Geophys. Res.* **2002**, *107*, Art. 8196.
(28) Li, J.; Dasgupta, P. K.; Luke, W. T. Measurement of Gaseous and Aqueous Trace Formaldehyde. Revisiting the Pentanedione Reaction and Field Applications**.** *Anal. Chim. Acta* **2005**, *531*, 51−68.
(29) Fried, A.; Crawford, J.; Olson, J.; Walega, J.; Potter, W.; Wert, B. P.; Jordan, C.; Anderson, B.; Shetter, R.; Lefer, B.; Blake, D.; Blake, N.; Meinardi, S.; Heikes, B. G.; O'Sullivan, D.; Snow, J.; Fuelberg, H.; Kiley, C. M.; Sandholm, S. Tan, D.; Sachse, G.; Singh, H.; Faloona, I.; Harward, C. N.; Carmichael, G. R. Airborne tunable diode laser measurements of formaldehyde during TRACE-P: Distributions and box model comparisons. *J. Geophys. Res.-Atmos.* **2003**, *108* (D20), Art. 8798.
(30) Wert, B. P.; Fried, A.; Rauenbuehler, S.; Walega, J.; Henry, B. Design and performance of a tunable diode laser absorption spectrometer for airborne formaldehyde measurements. *J. Geophys. Res.-Atmos.* **2003**, *108* (D12), Art. 4350.
(31) Ryerson, T. B.; Trainer, M.; Angevine, W. M.; Brock, C. A.; Dissly, R. W.; Fehsenfeld, F. C.; Frost, G. J.; Goldan, P. D.; Holloway, J. S.; Hubler, G.; Jakoubek, R. O.; Kuster, W. C.; Neuman, J. A.; Nicks, D. K., Jr.; Parrish, D. D.; Roberts, J. M.; Sueper, D. T.; Atlas, E. L.; Donnelly, S. G.; Flocke, F.; Fried, A.; Potter, W. T.; Schauffler, S.; Stroud, V.; Weinheimer, A. J.; Wert, B. P.; Wiedinmyer, C.; Alvarez, R. J.; Banta, R. M.; Darby, L. S.; Senff, C. J. Effect of petrochemical industrial emissions of reactive alkenes and NO_x on troposphheric ozone formation in Houston, TX. *J. Geophys. Res.* **2003**, *108* (D8), Art. 4249.
(32) Fried, A., Wang, Y.; Cantrell, C.; Wert, B. P.; Walega, J.; Ridley, B.; Atlas, E.; Shetter, R.; Lefer, B.; Coffey, M. T.; Hannigan, J.; Blake, D.; Blake, N.; Meinardi, S.; Talbot, R. W.; Dibb, J.; Scheuer, E.; Wingenter, O.; Snow, J.; Heikes, B. G.; Ehhalt, D. Tunable diode laser measurements of formaldehyde during the TOPSE 2000 study: Distributions, trends, and model comparisons. *J. Geophys. Res.* **2003**, *108* (D4), Art. 4104.
(33) Wert, B. P.; Fried, A.; Henry, B.; Cartier, S. Evaluation of inlets used for the airborne measurement of formaldehyde. *J. Geophys. Res.* **2002**, *107* (D13), Art. 4163.
(34) Perner, D.; Platt, U. Direct measurements of atmospheric formaldehyde, nitrous acid, ozone, nitrogen dioxide, and sulfur dioxide by differential optical absorption in the near UV. *J. Geophys. Res.* **1980**, *85*, 7453−7458.
(35) Stutz, J.; Platt, U. Improving long-path differential optical absorption spectroscopy with a quartz-fiber mode mixer. *Appl. Opt.* **1997**, *36*, 1105−1115.
(36) Harder, J. W.; Fried, A.; Sewell, S.; Henry, B. Comparison of tunable diode laser and long path ultraviolet/visible spectroscopic measurements of formaldehyde concentrations during the 1993 OH photochemistry experiment. *J. Geophys. Res.* **1997**, *102*, 6267−6282.
(37) Karl, T.; Jobson, T.; Kuster, W. C.; Williams, E.; Stutz, J.; Shetter, R.; Hall, S. R.; Goldan, P.; Fehsenfeld, F.; Lindinger, F. Use of proton-transfer-reaction mass spectrometry to characterize volatile organic compound sources at the La Porte supersite during the Texas Air Quality Study 2000. *J. Geophys. Res.* **2003**, *108*, Art. 4508.
(38) Lazrus, A. L.; Fong K. L.; Lind, J. A. Automated fluorometric determination of formaldehyde in air. *Anal. Chem.* **1988**, *60*, 1074−1078.
(39) Mücke R.; Scheumann, B.; Slemr, J.; Slemr, F.; Werle, P. Measurements of formaldehyde by tunable diode laser spectroscopy and the enzymatic fluorometric method: An intercomparison study. *Infrared Phys. Technol.* **1996**, *37*, 29−32.
(40) Fried, A.; Lee, Y.-N.; Frost, G.; Wert, B. P.; Henry, B.; Drummond, J. R.; Hübler, G.; Jobson, T. Airborne CH_2O measurements over the North Atlantic during the 1997 NARE campaign: Instrument comparisons and distributions. *J. Geophys. Res.* **2002**, *107* (D4), Art. 4039.
(41) Cardenas, L. M.; Brassington, D. J.; Allan, B. J.; Coe, H.; Alicke, B.; Platt, U.; Wilson, K. M.; Plane, J. M. C.; Penkett, S. A. Intercomparison of formaldehyde measurements in clean and polluted atmospheres. *J. Atmos. Chem.* **2000**, *37*, 53−80.
(42) http://www.aero-laser.de/html/home.html.
(43) Komazaki, Y.; Hiratsuka, M.; Narita, Y.; Tanaka, S.; Fujita, T. The development of an automated continuous measurement system for the monitoring of HCHO and CH_3CHO in the atmosphere by using an annular diffusion scrubber coupled to HPLC. *Fresenius' J. Anal. Chem.* **1999**, *363*, 686−695.
(44) Dasgupta, P. K.; Dong, S.; Hwang, H.; Yang, H.-C.; Genfa, Z. Continuous liquid-phase fluorometry coupled to a diffusion scrubber for the real-time determination of atmospheric formaldehyde, hydrogen peroxide and sulfur dioxide. *Atmos. Environ.* **1988**, *22*, 949−963.
(45) http://www.alphaomegapt.com/methanalyzer.htm.
(46) Kleindienst, T. E.; Shepson, P. B.; Nero, C. M.; Arnts, R. R.; Tejada, S. B.; MacKay, G. I.; Mayne, L. K.; Schiff, H. I.; Lind, J. A.; Kok, G. L.; Lazrus, A. L.; Dasgupta, P. K.; Dong, S. An intercomparison of formaldehyde measurement techniques at ambient concentrations. *Atmos. Environ.* **1988**, *22*, 1931−1939.
(47) Trapp, D.; DeServes, C. Intercomparison of formaldehyde measurements in the tropical atmosphere. *Atmos. Environ.* **1995**, *29*, 3239−3243.
(48) Zhang, G.; Dasgupta, P. K.; Cheng, Y.-S. Design of a straight inlet diffusion scrubber − Comparison of particle transmission with other collection devices and characterization for the measurement of hydrogen peroxide and formaldehyde. A*tmos. Environ.* **1991**, *25A*, 2717−2729.
(49) Fan, Q.; Dasgupta, P. K. Continuous automated determination of atmospheric formaldehyde at the parts per trillion level. *Anal. Chem.* **1994**, *66*, 551−556.
(50) Gilpin, T.; Apel, E.; Fried, A.; Wert, B.; Calvert, J.; Genfa, Z.; Dasgupta, P. K.; Harder, J. W.; Heikes, B. G.; Hopkins, B.; Westberg, H.; Kleindienst, T.; Lee, Y.-N.; Zhou, X.; Lonneman, W.; Sewell, S. Intercomparison of six ambient $[CH_2O]$ measurement techniques. *J. Geophys. Res.* **1997**, *102*, 21161−21188.
(51) Dasgupta, P. K. In *Sampling and Sample Preparation Techniques for Field and Laboratory*; Pawliszyn, J., Ed.; Wilson and Wilson's Comprehensive Analytical Chemistry Series, Vol. XXXVII, Elsevier: New York, 2002; pp 97−160.
(52) Dasgupta, P. K.; Zhang, G.; Li, J.; Boring, C. B.; Jambunathan, S.; Al-Horr, R. Luminescence detection with a liquid core waveguide. *Anal. Chem.* **1999**, *71*, 1400−1407.
(53) Li, J.; Dasgupta, P. K.; Genfa, Z.; Hutterli, M. A. Measurement of atmospheric formaldehyde with a diffusion scrubber and light-emitting diode-liquid-core waveguide based fluorometry. *Field Anal. Chem. Technol.* **2001**, *5*, 2−12.
(54) Röthlisberger, R. von Wassersoff, Peroxid and Formaldehyd in Atmosphäre and Firnluft. Diplomarbeit, University of Bern, Switzerland, 1996.
(55) Staffelbach, T.; Neftel, A.; Blatter, A.; Gut, A.; Fahrni, M.; Stahelin, J.; Prevot, A.; Hering, A.; Lehning, M.; Neininger, B.; Baumle, M.; Kok, G. L.; Dommen, J.; Hutterli, M.; Ankin, M. Photochemical oxidant formation over southern Switzerland 0.1. Results from summer 1994. *J. Geophys. Res.* **1997**, *102*, *23*, 345.
(56) Hutterli, M. Luft-Firn Transferstudien von HCHO und H_2O_2 zur Interpretation von Eisbohrkerndaten. Ph.D. Dissertation, University of Bern, Switzerland, 1999.
(57) de Serves, C. Gas phase formaldehyde and peroxide measurements in the arctic atmosphere. *J. Geophys. Res.* **1994**, *99*, 25391−25398.
(58) Hutterli, M. A.; Röthlisberger, R.; Bales, R. C. Atmosphere-to-snow-to-firn transfer studies of HCHO at Summit, Greenland. *Geophys. Res. Lett.* **1999**, *26*, 1691−1694.
(59) Dasgupta, P. K. Loree, E. L.; Li, J.; Genfa, Z. *Anal. Chem.* **2003**, *75*, 3924−3928.
(60) http://www.al.noaa.gov/WWWHD/pubdocs/SOS/sos99.groundsites.html.
(61) http://www.al.noaa.gov/WWWHD/pubdocs/SOS/sos99.doas.html#doas.
(62) http://www.tnrcc.state.tx.us/cgi-bin/monops/daily_summary?603.
(63) Stutz, J., Alicke, B. Ackermann, R.; Geyer, A.; White, A.; Williams, E. Vertical profiles of NO_3, N_2O_5, O_3, and NO_x in the nocturnal boundary layer: 1. Observations during the Texas Air Quality Study 2000. *J. Geophys. Res.* **2004**, *109*, Art. 12306.
(64) Li, J.; Dasgupta, P. K.; Tarver, G. A. Pulsed excitation source multiplexed fluorometry for the simultaneous measurement of multiple analytes. Continuous measurement of atmospheric hydrogen peroxide and methyl hydroperoxide. *Anal. Chem.* **2003**, *75*, 1203−1210.
(65) Boring, C. B.; Al-Horr, R.; Genfa, Z.; Dasgupta, P. K.; Martin, M. W.; Smith, W. F. Field measurement of acid gases and soluble anions in atmospheric particulate matter using a parallel plate

wet denuder and an alternating filter-based automated analysis system. *Anal. Chem.* **2002**, *74*, 1256−1268.
(66) Al-Horr, R.; Samanta, G.; Dasgupta, P. K. A continuous analyzer for soluble anionic constituents and ammonium in atmospheric particulate matter. *Environ. Sci. Technol.* **2003**, *37*, 5711−5720.
(67) Wiesen, P. Nitrous Acid and its Influence on the Oxidation Capacity of the Atmosphere (NITROCAT), Final Report, October 2003. http://www.physchem.uni-wuppertal.de/PC-WWW_Site/Publications/Publications.html.
(68) Possanzini, M.; Di Palo, V.; Cecinato, A. Sources and photodecomposition of formaldehyde and acetaldehyde in Rome ambient air. *Atmos. Environ.* **2002**, *36*, 3195−3201.
(69) Possanzini, M.; Di Palo, V.; Petricca, M.; Fratarcangeli, R.; Brocco, D. Measurements of lower carbonyls in Rome ambient air. *Atmos. Environ.* **1996**, *30*, 3757−3764.
(70) Bakeas, E. B.; Argyris, D. I.; Siskos, P. A. Carbonyl compounds in the urban environment of Athens, Greece. *Chemosphere* **2003**, *52*, 805−813.
(71) Correa, S. M.; Martins, E. M.; Arbilla, G. Formaldehyde and acetaldehyde in a high traffic street of Rio de Janeiro, Brazil. *Atmos. Environ.* **2003**, *37*, 21−29.
(72) Cowling, E. B.; Chameides, W. L.; Kiang, C. S.; Fehsenfeld, F. C.; Meagher, J. F. Introduction to special section: Southern Oxidants Study Nashville/middle Tennessee ozone study, Part 2. *J. Geophys. Res.* **2000**, *105* (D7), 9075−9077.
(73) Kleinman, L. I.; Daum, P. H.; Imre, D. G.; Cardelino, C.; Olszyna, K. J.; Zika, R. G. Trace gas concentrations and emissions in downtown Nashville during the 1995 Southern Oxidants Study Nashville intensive. *J. Geophys. Res.* **1998**, *103*, *22*545−22553.
(74) Solomon, P. A.; Chameides, W.; Weber, R.; Middlebrook, A.; Kiang, C. S.; Russell, A. G.; Butler, A.; Turpin, B.; Mikel, D.; Scheffe, R.; Cowling, E.; Edgerton, E.; St. John, J.; Jansen, J.; McMurry, P.; Hering, S.; Bahadori, T. Overview of the 1999 Atlanta supersite project. *J. Geophys. Res.* **2003**, *108*, (D7), Art. 8413.
(75) See, e.g., http://www.smokemup.com/tech/fuels.php.
(76) Field intercomparison of a novel optical sensor for formaldehyde quantification. Friedfeld, S.; Fraser, M.; Lancaster, D.; Leleux, D.; Rehle, D.; Tittel, F. *Geophys. Res. Lett.* **2000**, *27*, 2093−2096.
(77) Rehle, D.; Leleux, D.; Erdelyi, M.; Tittel, F.; Fraser, M.; Friedfeld, S. Ambient formaldehyde detection with a laser spectrometer based on difference-frequency generation in PPLN. *Appl. Phys. B* **2001**, *72* (8), 947−952.
(78) Watson, T. B.; Luke, W. T.; Arnold, J. R.; Gunter, L. R. Studies of Tampa Bay region power plant plumes during the Bay Region Atmospheric Chemistry Experiment (BRACE). *EOS, Trans. Am. Geophys. Union* **2003**, *84* (46), *Fall Meet. Suppl.*, Abstract A51A-08.
(79) Arlander, D. W.; Bruning, D.; Schmidt, U.; Ehhalt, D. H. The tropospheric distribution of formaldehyde during TROPOZ-II. *J. Atmos. Chem.* **1995**, *22*, 251−269.
(80) Heikes, B.; Snow, J.; Egli, P.; O'Sullivan, D.; Crawford, J.; Olson, J.; Chen, G.; Davis, D.; Blake, N.; Blake, D. Formaldehyde over the central Pacific during PEM-Tropics B. *J. Geophys. Res.* **2001**, *106*, 32, 717−32, 731.
(81) Kormann, R.; Fischer, H.; de Reus, M.; Lawrence, M.; Brühl, Ch.; von Kuhlmann, R.; Holzinger, R.; Williams, J.; Lelieveld, J.; Warneke, C.; de Gouew, J.; Heland, J.; Zierels, H.; Schlager, H. Formaldehyde over the eastern Mediterranean during MINOS: Comparison of airborne in-situ measurements with 3-D model results. *Atmos. Chem. Phys.* **2003**, *3*, 851−861.

Received for review October 26, 2004. Revised manuscript received March 29, 2005. Accepted April 29, 2005.

ES048327D